

Chapter V. BAE Cell System Models

Mathematical modeling provides a means for scientists and engineers to assess preliminary data and design future experiments. Model development can facilitate and shorten experimentally time-consuming analysis of specific parameter effects. Cell behavior and response can be predicted with a mathematical model and later be tested experimentally. For example, it would be valuable to correlate IGF-I/IGF-IR binding with levels of exogenous IGFBP-3 and p9 HS added to the system. The model is developed specifically for the IGF-I/IGF-IR, IGFBP-3 and p9 HS system, however, it can be applied to different biological systems once parameter measurements for different IGFbps or growth factors are obtained. Mathematical models have been used previously for autocrine systems exploring the effects of inoculum cell density on cell growth⁶⁷ and predicting autocrine ligand secretion effects on ligand-receptor surface binding⁶⁸ along with other ligand-receptor phenomena⁶⁹.

A mathematical model can incorporate chemical engineering topics such as transport phenomena, chemical kinetics and numerical analysis. For example, the ligand must diffuse through the bulk fluid medium for which a transport is characterized by a diffusion coefficient. Ligand transport may be helped or hindered by soluble receptors present in the bulk fluid medium. Kinetic expressions can be written for the association and dissociation rates of the ligand to the receptors (surface and soluble). The change in unbound and bound ligand and receptors (surface and soluble) can be characterized by time derivatives with no spatial dependence.

The mathematical model is based on the idea that the behavior of a distinct molecule does not happen in isolation. The interactions of different components in the system provide the driving force for cellular activity. For example, the binding and internalization of IGF-I would result in a decrease in the local concentration of IGF-I close to the cell surface which may induce up-regulation of IGF-IR on the cell surface. However, binding between IGF-I and IGF-IR may cause a significant decrease in the number of IGF-IR on the cell surface if the rate of internalization of IGF-I/IGF-IR complexes is larger than the rate of synthesis of new IGF-IR. It is important to note that the variables in the system; IGF-I in solution, unbound cell surface receptors, IGFBP-3 and p9 HS concentrations, are related to each other and it should be possible to write

kinetic expressions relating the change with respect to time. Evaluation of the model will allow for the investigation of how individual parameters affect the system of variables. The rates of association and dissociation must be considered as well as the overall equilibrium constants for each molecular reaction in the system. Simple steady state analysis or transient analysis can be used in evaluating the effects IGFBP-3 and p9 HS have on IGF-I/IGF-IR binding.

A. BAE Cell System Models

The mathematical models presented are based on a model previously developed by Forsten and Lauffenberger^{70,71}. A homogenous distribution of spherical suspension cells of radius a form the basis for the model. This assumption simplifies the model by assuming that cells are in suspension rather than plated. There are important discrepancies between plated cell and suspension cell models. Suspension cells have a homogenous bulk medium where cell to cell communication occurs. Plated cells have an additional intermediate boundary layer that surrounds and connect the cells. The transport of ligand and soluble receptors (IGFBP-3 and p9 HS) may be interrupted by the presence of the intermediate boundary layer⁷². The suspension model does not account for this interruption. The diffusion within the bulk medium of the cell would be distinguished by the Smoluchowski diffusion-controlled rate constant for a hemisphere instead of a sphere in plated cells, ensuing a reduced transport coefficient for plated cells⁷³. The growth rate of cells can be affected by surface geometry. For example, higher critical inoculum densities are necessary for spherical cells versus plated cells⁷⁴. Many autocrine systems involve cell types that will not grow in suspension and are anchorage-dependent, however, Forsten and Lauffenberger⁷⁰ have found that fundamental model results were independent of the geometric structure of the system.

IGF-IR are assumed to be uniformly disbursed on the cell surface. No ligand secretion, receptor synthesis or internalization (constitutive or ligand-induced) is included as the model is being based on experiments done at 4°C which typically prevent protein synthesis and receptor trafficking. IGF-I/IGF-IR binding is reversible with on and off rates denoted as k_{on} and k_{off} . The forward (k_{for}) and reverse (k_{rev}) rate constants account for competing receptor effects and are a function of both the intrinsic k_{on} and k_{off} and the free receptor concentration. The overall equilibrium constant K_D (K_D)

$= k_{\text{rev}} / k_{\text{for}}$) for IGF-I/IGF-IR was obtained from literature as 0.2-1 nM³⁷. IGF-I binding with IGFBP-3 or p9 HS is reversible with on and off rates denoted as k_{on} and k_{off} . The overall equilibrium constant K_D ($K_D = k_{\text{off}} / k_{\text{on}}$) was obtained with a least squares analysis of biodot assay and charcoal assay data, (Appendix A). The charcoal assay was used for determining K_D . The K_D values were similar for both biodot and charcoal assays for both IGF-I/p9 HS and IGF-I/IGFBP-3 and are presented in Table 5-1. Free IGF-I pinocytosis and IGF-IR recycling are disregarded as secondary effects.

Table 5-1 Experimental Binding Affinities

	Biodot Assay Binding Affinity, K_D (M)	Charcoal Assay Binding Affinity, K_D (M)
IGF-I/IGFBP-3	6.2 x 10 ⁻⁹ M	3.0 x 10 ⁻⁹ M
IGF-I/p9 HS	2.2 x 10 ⁻⁷ M	1.5 x 10 ⁻⁸ M

Basic BAE Cell System Model:

The Basic BAE Cell System Model is a simplified version of an *in vitro* cell system. This model is based on IGF-I/IGF-IR binding only and does not allow for exogenous IGFBP-3 or p9 HS, (Figure 5-1).

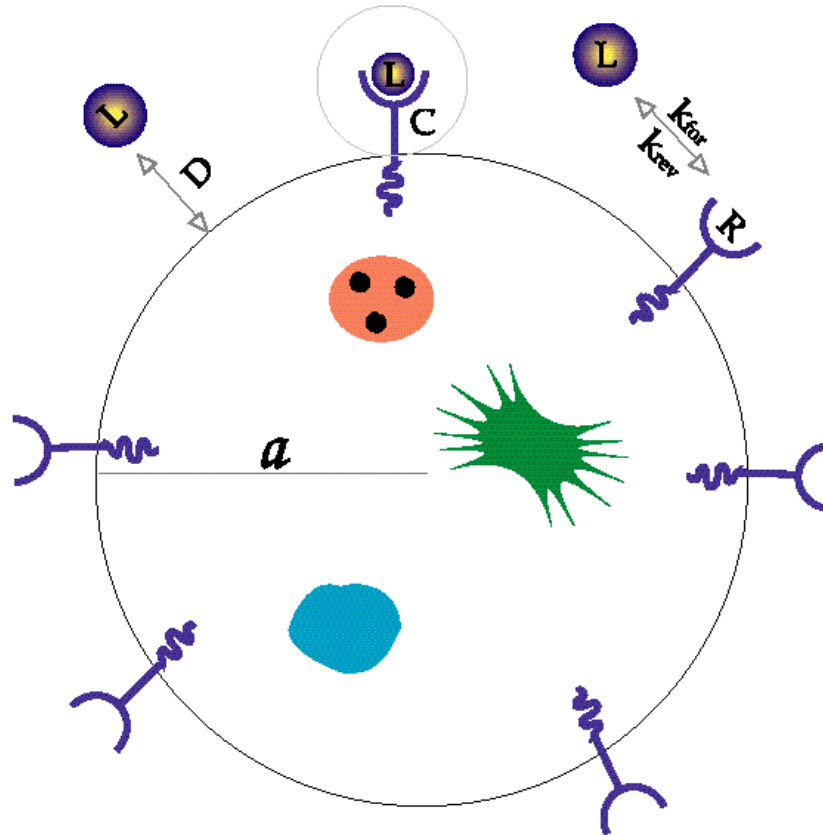


Figure 5-1 Schematic illustration of Basic BAE Cell System Model. All variables and parameters shown on the model are described by symbol in the text.

The transient expressions for the change in unoccupied and occupied IGF-IR, R and C respectively, are:

$$dR/dt = -k_{for} [L][R] + k_{rev} [C], \quad (1)$$

$$dC/dt = k_{for} [L][R] - k_{rev} [C], \quad (2)$$

Only ligand-receptor binding is included with no allowance for receptor-IGFBP-3 or receptor-p9 HS binding. In addition, no IGF-I/IGFBP-3 or IGF-I/p9 HS complexes are permitted to bind to the cell surface receptors. The transient expression for the change in solution IGF-I is:

$$VdL/dt = -k_{for}[L][R] + k_{rev}[C]. \quad (3)$$

No secretion, degradation or internalization of free IGF-I and IGF-IR is included, (Table 5-2).

Table 5-2 Basic BAE Cell System Model Equations
$dR/dt = -k_{for}[L][R] + k_{rev}[C]$
$dC/dt = k_{for}[L][R] - k_{rev}[C]$
$V(dL/dt) = -k_{for}[L][R] + k_{rev}[C]$
where $k_{for} = k_{on}/(1+(k_{on}R/4 aD))$ and $k_{rev} = k_{off}/(1+(k_{on}R/4 aD))$

The effect of competing receptors were taken into account with the forward and reverse rate constants, k_{for} and k_{rev} . Briefly, the expressions used for k_{for} and k_{rev} are:

$$k_{for} = k_{on}/(1+(k_{on}R/4 aD)) \quad (4)$$

$$k_{rev} = k_{off}/(1+(k_{on}R/4 aD)) \quad (5)$$

System values and parameters and initial conditions for the Basic BAE Cell System Model are shown in Table 5-3.

Table 5-3 Basic BAE Cell System Model Parameters and Equations

<i>Parameter Values</i>		
K_D	$.6 \times 10^{-9} \text{ M}$	Jones and Clemmons, 1995
k_{on}	$4 \times 10^7 \text{ M}^{-1}\text{s}^{-1}$	Forsten and Lauffenberger, 1992
R_o	$2 \times 10^4 \text{ receptors/cell}$	Forsten and Lauffenberger, 1992
a	$5 \times 10^{-4} \text{ cm}$	Forsten and Lauffenberger, 1992
D	$5 \times 10^{-7} \text{ cm}^2/\text{s}$	Geankopolis, 1993
V	$3.33 \times 10^{-5} \text{ cm}^3/\# \text{ of cells}$	Experimental
L_o	$5.7 \times 10^{-10} \text{ M}$	Experimental
<i>Initial Conditions</i>		
R/R_o	1.0	all receptors initially unbound
C/R_o	0.0	no initial complexes
L/K_D	L_o/K_D	

Prior to time zero ligand and receptors are unbound. The association rate constant (k_{on}) for IGF-I/IGF-IR binding was varied and the dissociation rate constant (k_{off}) for IGF-I/IGF-IR binding was determined as a function of k_{on} and K_D . The diffusion coefficient for the ligand was estimated based on the molecular weight of IGF-I using a semi-empirical equation for biological solutes in aqueous solutions:

$$D = 5 \times 10^{-7} \text{ cm}^2/\text{s}^{75}$$

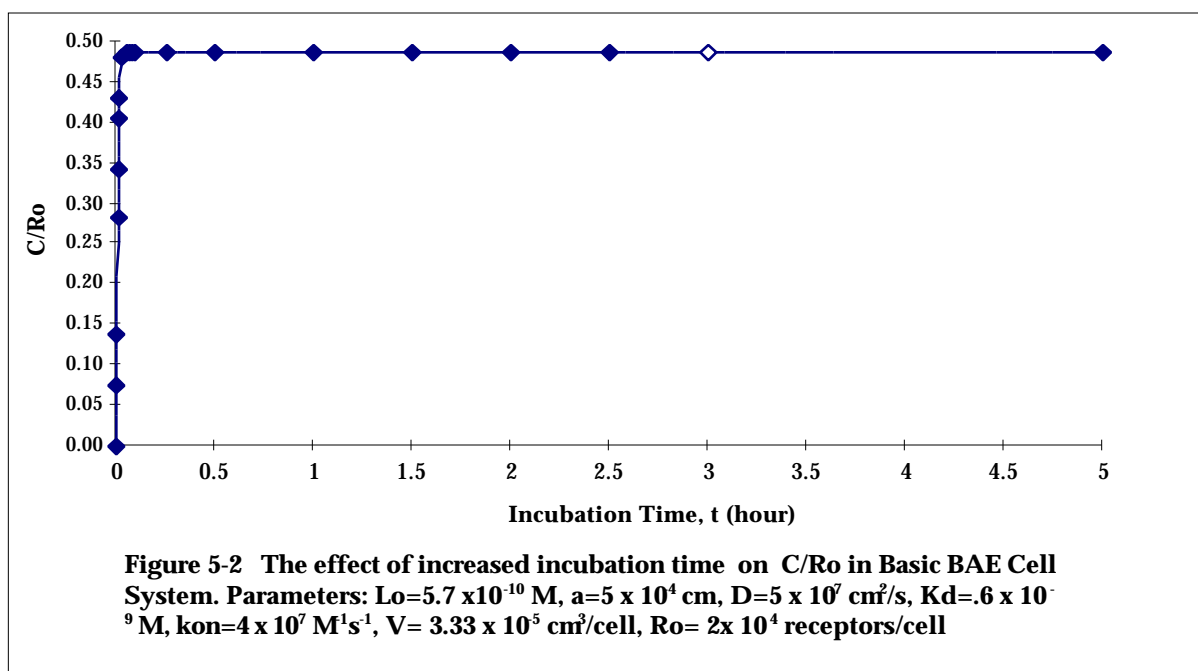
The radius of the BAE cell is based on a generic value for spherical cells of uniform distribution:

$$a = 5 \times 10^{-4} \text{ cm}^{70}$$

The computer subroutine LSODE, an implicit solver, was used to solve the system of linear ordinary differential equations^{68,70}. The FORTRAN (Microsoft FORTRAN Compiler 3.2) program used can be found in Appendix B. Results for the

Basic BAE Cell System Model are presented as a ratio of the cell surface receptor-ligand complexes (C) to initial unbound receptors (Ro) present on the cell surface as C/Ro. C/Ro represents ligand-receptor surface complexes. Most results are presented on a logarithmic scale. Base system parameters are denoted by an open diamond.

Initial analysis of the Basic BAE Cell System Model was performed with a range of time periods ranging from 0-5 hours, (Figure 5-2). The system reaches steady state in six minutes clearly faster than what is seen experimentally. This may be due to the optimum conditions the computer simulated model is based on. The experimental binding studies can be affected by environmental conditions, human error and other cell affects that are neglected in the model for simplicity.



The remainder of the Basic BAE Cell System Model analysis was done at a time period of 3 hours (steady state) and initial ligand concentration (L_0) of 5.7×10^{-10} M. These conditions were chosen to mimic experimental binding studies done in the laboratory, (See Section 2.J).

The Basic BAE Cell System Model is insensitive to cell radius (a) and ligand diffusivity (D) parameters. Figure 5-3 shows that varying the cell radius by several orders of magnitude has no effect on ligand-receptor surface complexes as represented by C/R_o . Likewise, varying ligand diffusivity by several orders of magnitude did not affect C/R_o , (Figure 5-4) This is expected due to the small role that these parameters play in the overall scheme of equations.

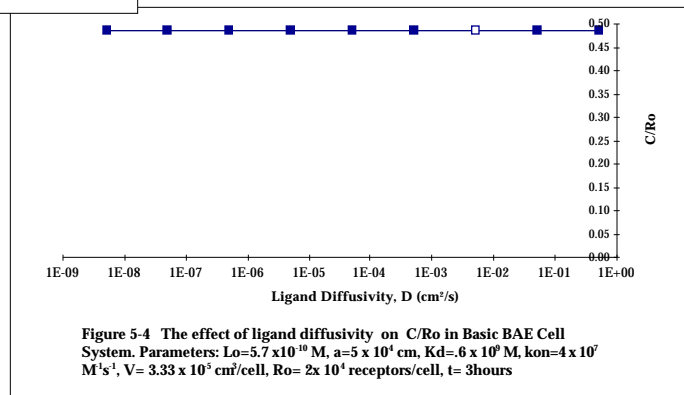
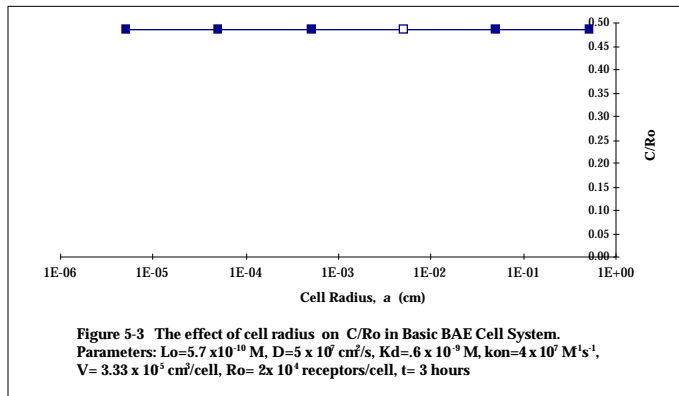
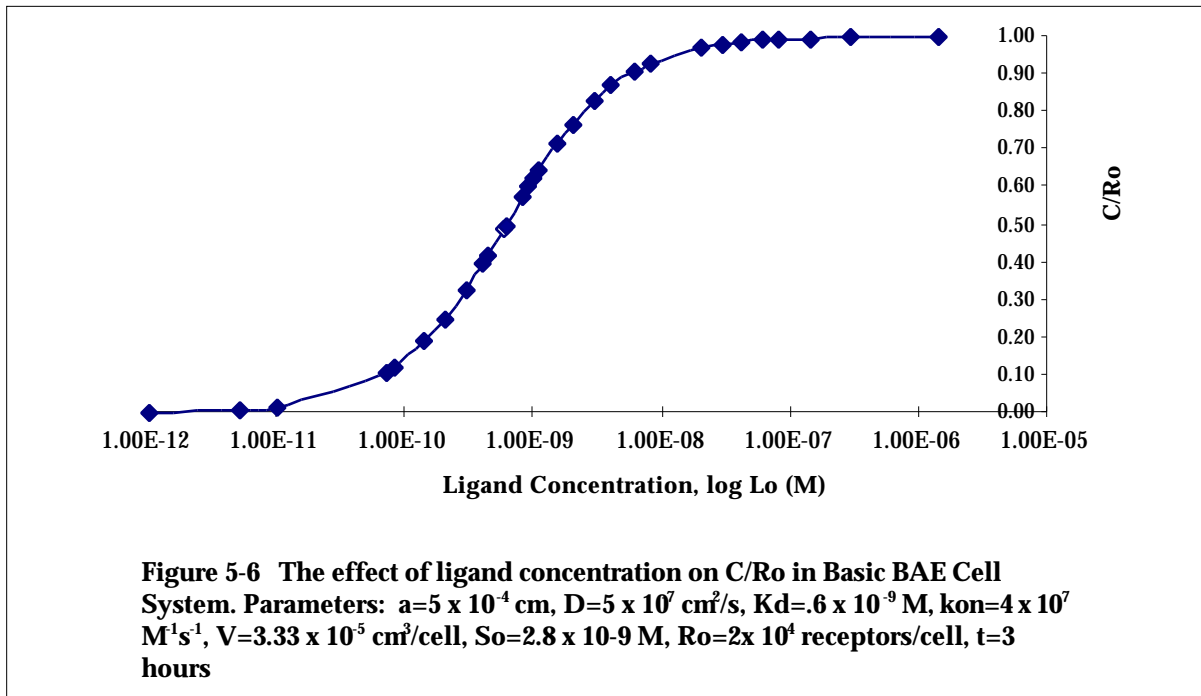
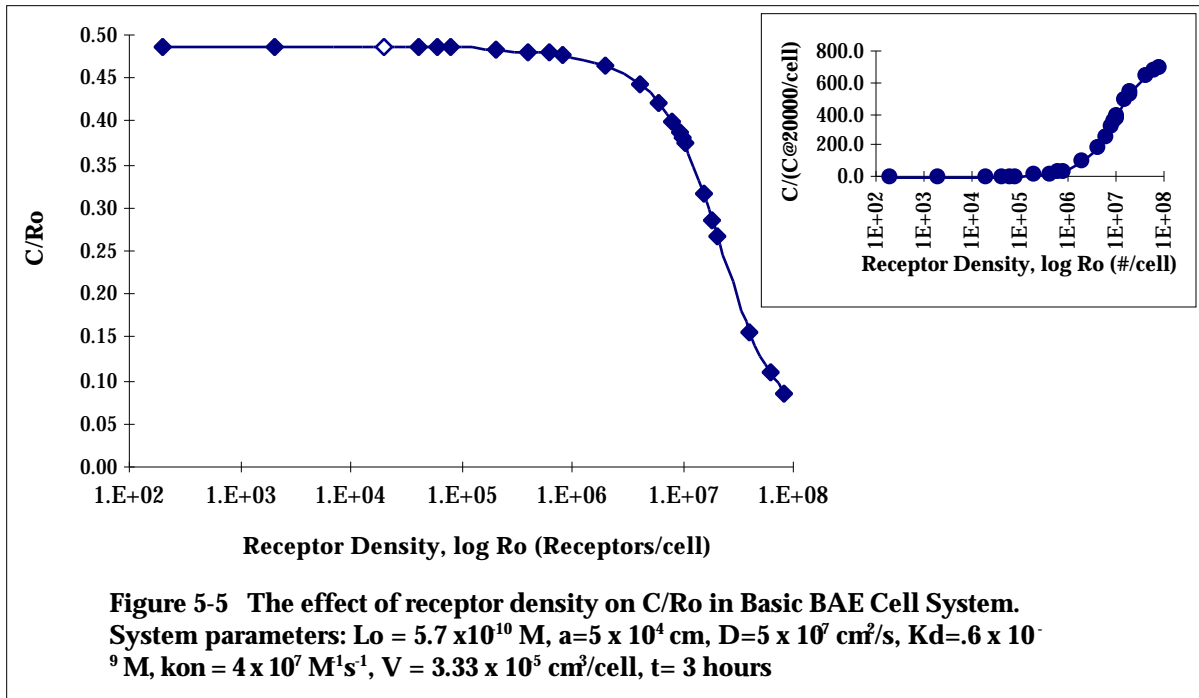


Figure 5-5 shows that as the number of available receptors on the cell surface increases from 2×10^2 - 8×10^7 receptors/cell, C/R_o decreases by half. The decrease of C/R_o does not begin until cell receptor density reaches 2×10^6 receptors/cell with a half maximal decrease at a receptor density of 2×10^7 receptor/cell. The insert shows that the model results in Figure 5-5 do not represent a drop in the level of surface complexes (C), but instead, in the ratio of surface complexes to receptor density (C/R_o)

The effect of ligand concentration (L_o) on C/R_o is presented in Figure 5-6. Few surface complexes are predicted at very low ligand concentrations (1×10^{-12} M - 1×10^{-11}

M). C/R_o increases as L_o increases from 7.1×10^{-11} M to 8×10^{-9} M with a half-maximal increase occurring when ligand concentration is 6×10^{-10} M. The increase levels off at molar concentrations exceeding 2×10^{-9} M when all receptors are bound.



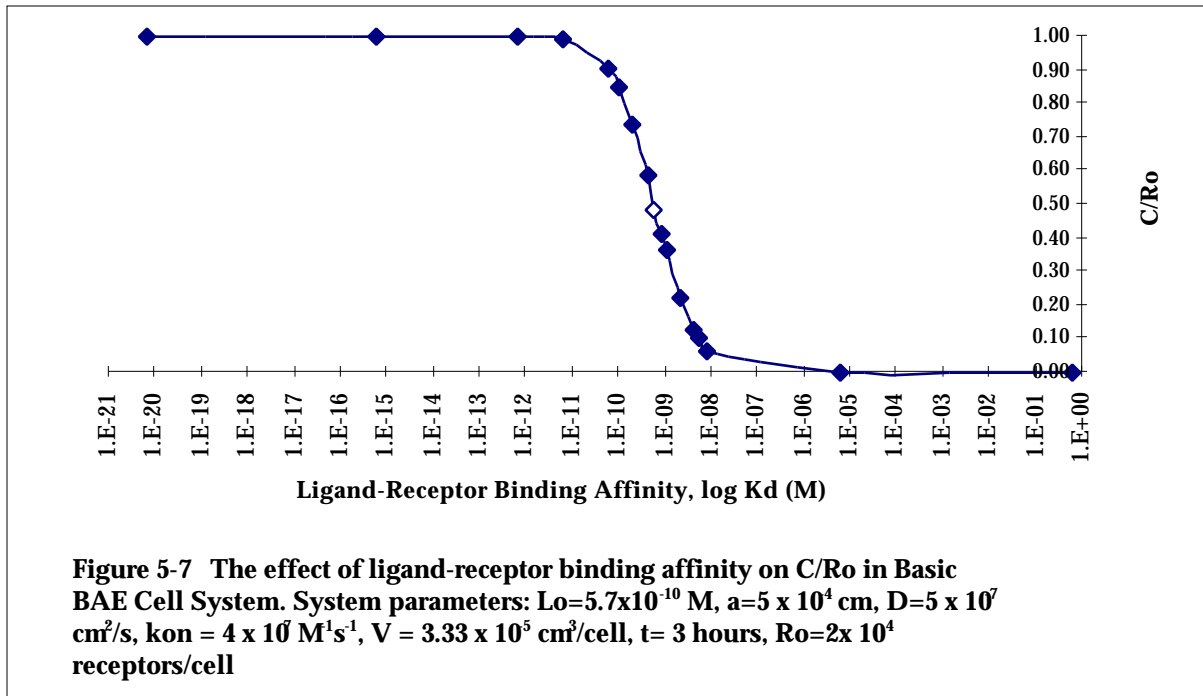
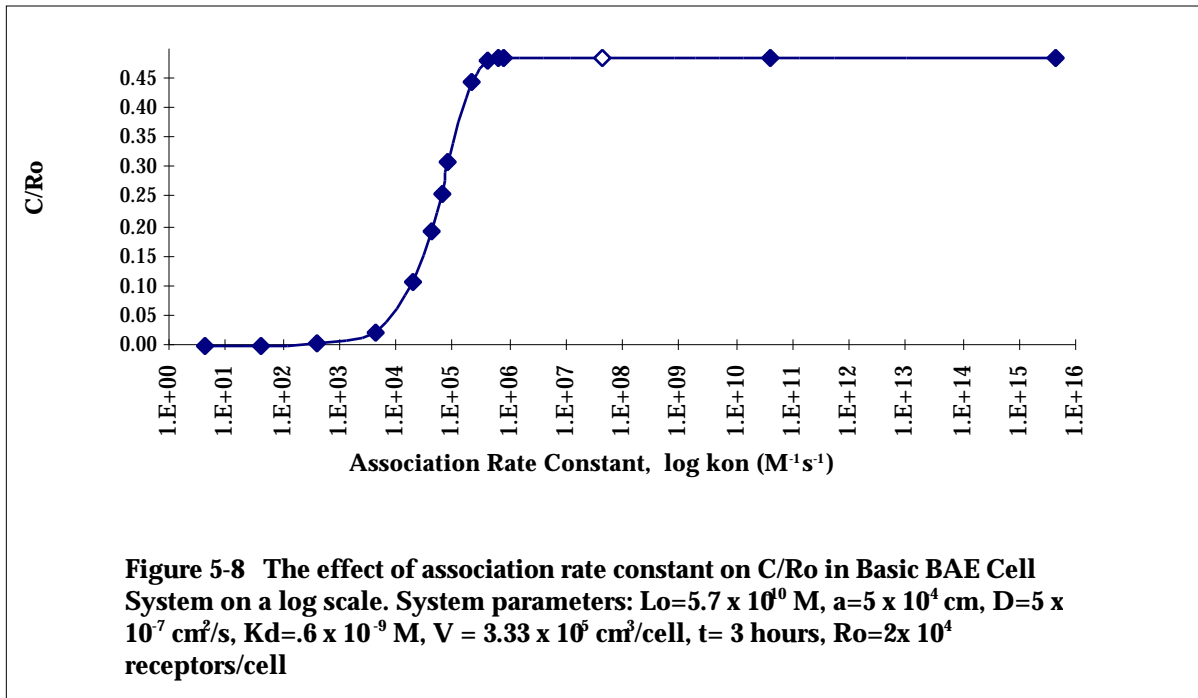


Figure 5-7 demonstrates the effect of ligand-receptor binding affinity (K_D) on C/R_0 . As K_D increases from 6×10^{-21} M to 6×10^{-12} M, C/R_0 does not change. C/R_0 starts to decrease at 6×10^{-11} M. A half-maximal decrease occurs at a K_D value of 5×10^{-10} M. Very few surface complexes are predicted at 6×10^{-6} M. A high affinity between molecules is when k_{on} must be much larger than k_{off} , which yields a very low value for K_D . As K_D increases, either k_{on} is decreasing or k_{off} is increasing resulting in less surface complexes.

Figure 5-8 shows the effect of the variation of the association rate constant, k_{on} ($4 - 4 \times 10^{15}$ M⁻¹s⁻¹) on C/R_0 while maintaining a constant K_D . As expected, at low association rate constants, k_{on} , C/R_0 is very low also. Few surface complexes are predicted between k_{on} values of $4 - 4 \times 10^2$ M⁻¹s⁻¹. Surface complexes may form at the low k_{on} values, but dissociate quickly. This may be due to corresponding high dissociation rate constants (k_{off}) at high association rate constants. C/R_0 starts to increase gradually at an association rate constant, k_{on} , of 4×10^3 M⁻¹s⁻¹ and continues through 2×10^5 M⁻¹s⁻¹. The increase plateaus at 4×10^7 M⁻¹s⁻¹. The half-maximal increase occurs at 6×10^4 M⁻¹s⁻¹.



The Basic BAE Cell System Model predicted a “no frills” system of IGF-I/IGF-IR binding in the absence of soluble receptors. The increase in receptor density, R_0 , and the equilibrium constant, K_D , results in a decrease of C/R_0 . Increasing receptor density increases ligand-receptor surface complexes, as shown in the inset of Figure 5-5 (complexes normalized by the complexes with 2×10^4 receptors/cell), but decreases C/R_0 . This decrease in C/R_0 may be due to the depletion of free ligand in the medium as receptor density increases. With the exception of varying receptor density, a decrease of C/R_0 will usually represent less ligand-receptor surface complexes and an increase of C/R_0 represents more ligand-receptor surface complexes. The increase in the equilibrium constant (decrease in ligand-receptor affinity), K_D , results in a decrease of C/R_0 . Likewise, an increase in the ligand-receptor association rate constant, k_{on} , results in an increase of ligand-receptor surface complexes. An increase in ligand concentration, L_0 , results in an increase of ligand-receptor surface complexes. Increasing ligand concentration would result in increased IGF-I/IGF-IR binding, however, down-regulation of surface receptors may occur when exposed to a large bolus of ligand due to the requirements of the cell for ligand. If receptor down-regulation was accounted for in the Basic BAE Cell System Model, there may not be as significant of an increase of C/R_0 in response to increasing ligand concentration with a plateau at much lower concentrations of ligand. The system reaches steady state in six minutes.

IGF-I/IGFBP-3 BAE Cell System Model:

The IGF-I/IGFBP-3 BAE Cell System Model is a more complex version of the Basic BAE Cell System Model due to the addition of IGFBP-3 into the system. This model is based on IGF-I/IGF-IR binding and IGF-I/IGFBP-3 binding, (Figure 5-9).

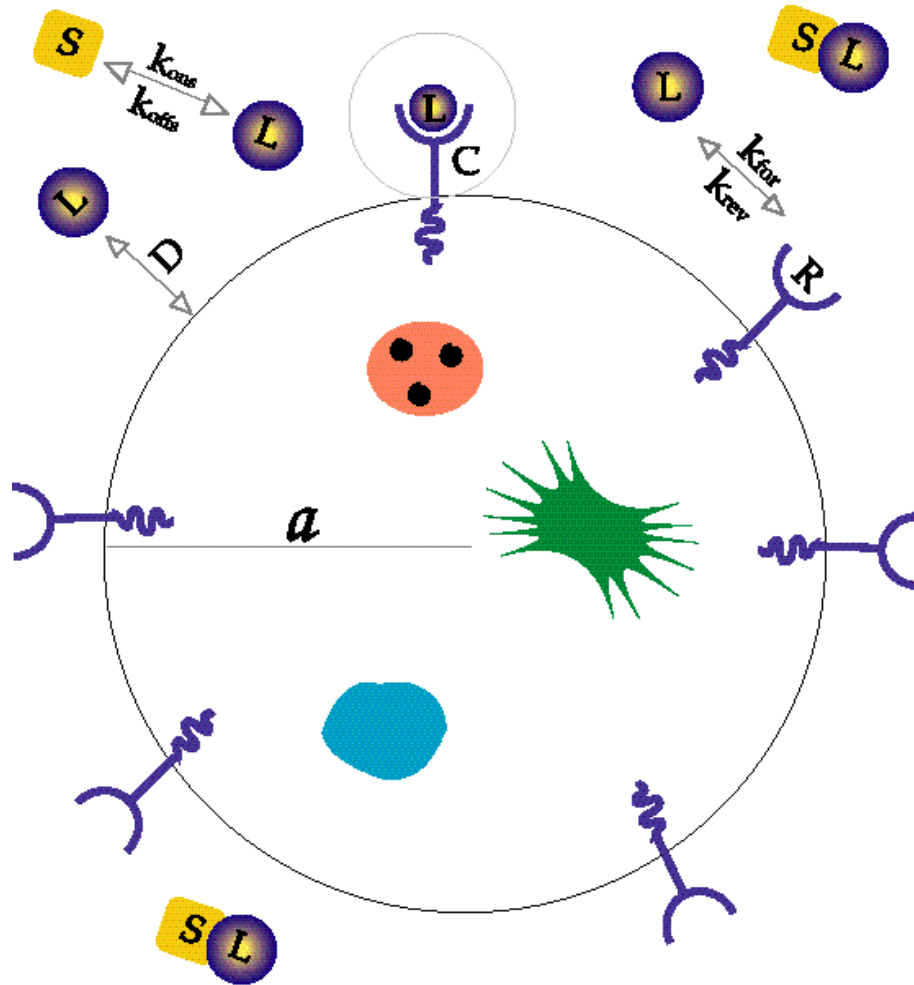


Figure 5-9 Schematic illustration of IGF-I/IGFBP-3 BAE Cell System Model. All variables and parameters shown on the model are described by symbol in the text.

The transient expressions for the model are presented in Table 5-4. The expressions are similar to the Basic BAE Cell System Model with the inclusion of IGFBP-3 as a soluble receptor. The change in free ligand concentration is a more intricate expression and new equations are introduced that represent the change in bound and unbound soluble

receptors where S and X are the free IGFBP-3 and IGF-I/IGFBP-3 complexes, respectively. These are as follows:

$$VdS/dt = -k_{on}^s[L][S] + k_{off}^s[X], \quad (6)$$

$$VdX/dt = k_{on}^s[L][S] - k_{off}^s[X], \quad (7)$$

$$VdL/dt = -k_{for}[L][R] + k_{rev}[C] - k_{on}^s[L][S] + k_{off}^s[X], \quad (8)$$

with k_{for} and k_{rev} as shown previously in Equation 4 and Equation 5. Regular association and dissociation rate constants, k_{on}^s and k_{off}^s are used for IGF-I/IGFBP-3 binding instead of k_{for} and k_{rev} , as used for IGF-I/IGF-IR binding. In solution, there is not the same clustering effect of competing receptors as on the cell⁷². No binding of IGFBP-3 with IGF-IR or any other cellular surface component is included.

Table 5-4 IGF-I/IGFBP-3 BAE Cell System Model Equations
$dR/dt = -k_{for}[L][R] + k_{rev}[C]$
$dC/dt = k_{for}[L][R] - k_{rev}[C]$
$V(dL/dt) = -k_{for}[L][R] + k_{rev}[C] - V k_{on}^s[L][S] + V k_{off}^s[X]$
$V(dS/dt) = -V k_{on}^s[L][S] + V k_{off}^s[X]$
$V(dX/dt) = V k_{on}^s[L][S] - V k_{off}^s[X]$
where $k_{for} = k_{on} / (1 + (k_{on} R / 4 aD))$ and $k_{rev} = k_{off} / (1 + (k_{on} R / 4 aD))$

System values and parameters and initial conditions are shown in Table 5-5. The association rate constant (k_{on}) for IGF-I/IGF-IR binding was varied and the dissociation rate constant (k_{off}) for IGF-I/IGF-IR binding was determined as a function of k_{on} and K_D . The association rate constant (k_{on}^s) for IGF-I/IGFBP-3 binding was varied and the dissociation rate constant (k_{off}^s) for IGF-I/IGFBP-3 binding was determined as a function of k_{on}^s and K_D^s .

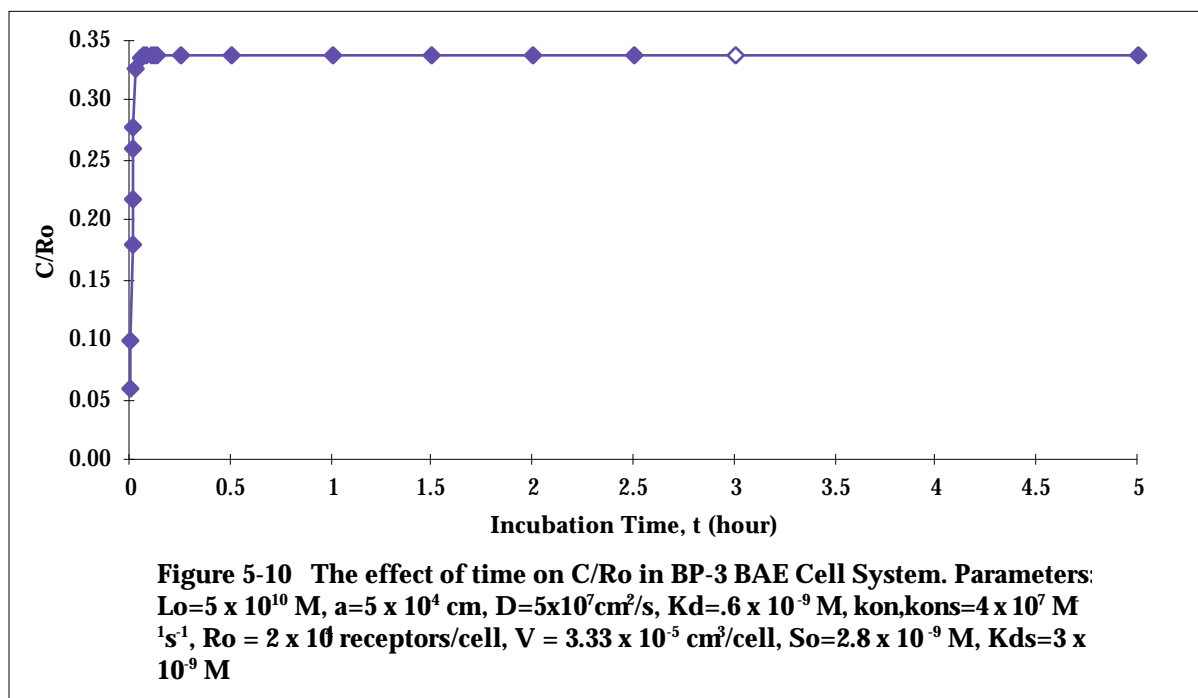
Table 5-5 IGF-I/IGFBP-3 BAE Cell System Model Equations

<i>Parameter Values</i>		
K_D	$.6 \times 10^{-9} \text{ M}$	Jones and Clemmons, 1995
k_{on}	$4 \times 10^7 \text{ M}^{-1}\text{s}^{-1}$	Forsten and Lauffenberger, 1992
K_D^s	$3 \times 10^{-9} \text{ M}$	Experimental
k_{on}^s	$4 \times 10^7 \text{ M}^{-1}\text{s}^{-1}$	Forsten and Lauffenberger, 1992
R_o	$2 \times 10^4 \text{ receptors/cell}$	Forsten and Lauffenberger, 1992
a	$5 \times 10^{-4} \text{ cm}$	Forsten and Lauffenberger, 1992
D	$5 \times 10^{-7} \text{ cm}^2/\text{s}$	Geankopolis, 1993
V	$3.33 \times 10^{-5} \text{ cm}^3/\# \text{ of cells}$	Experimental
L_o	$5.7 \times 10^{-10} \text{ M}$	Experimental
S_o	$2.8 \times 10^{-9} \text{ M}$	Experimental
<i>Initial Conditions</i>		
R/R_o	1.0	all receptors initially unbound
C/R_o	0.0	no initial complexes
L/K_D	L_o/K_D	
S/S_o	1.0	homogeneously distributed soluble receptors
X/S_o	0.0	no initial complexes

The FORTRAN program used for the IGF-I/IGFBP-3 BAE Cell System Model can be found in Appendix B. Results for the IGF-I/IGFBP-3 BAE Cell System Model are presented as a ratio of the ligand-receptor cell surface complexes (C) unbound receptors

(Ro) present in the system as C/R_o . Most results are presented on a log scale. Base system parameters are denoted with an open diamond.

Initial analysis of the IGF-I/IGFBP-3 BAE Cell System Model was performed with a range of time periods ranging from 0-5 hours, (Figure 5-10). The system reaches steady state in seven minutes. As seen with the Basic BAE Cell System Model, this is much faster than seen experimentally. This may be due to neglected cell system effects such as possible IGFBP-3 surface binding, secretion or degradation of IGF-I and IGF-IR. Also, the assumption of a well-mixed system may account for some discrepancies between experimental steady state and model steady state.



The remainder of the IGF-I/IGFBP-3 BAE Cell System Model analysis was done for a time period of 3 hours (steady state), initial ligand concentration (L_o) of 5.7×10^{-10} M and IGFBP-3 (S_o) concentration of 2.8×10^{-9} M. These were chosen to mimic experimental conditions, (See Section 2.J). The system is insensitive to cell radius and ligand diffusivity, (Figure 5-11, Figure 5-12).

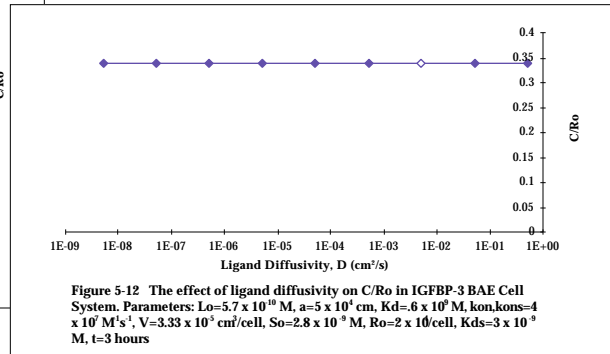
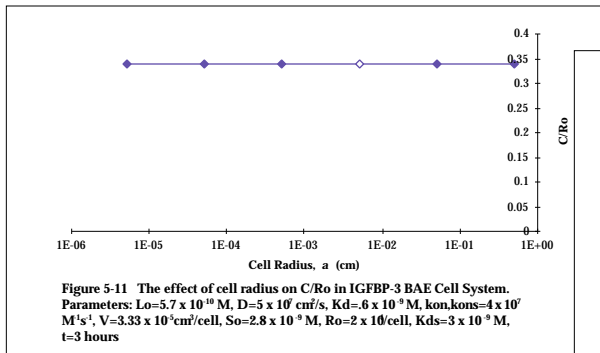
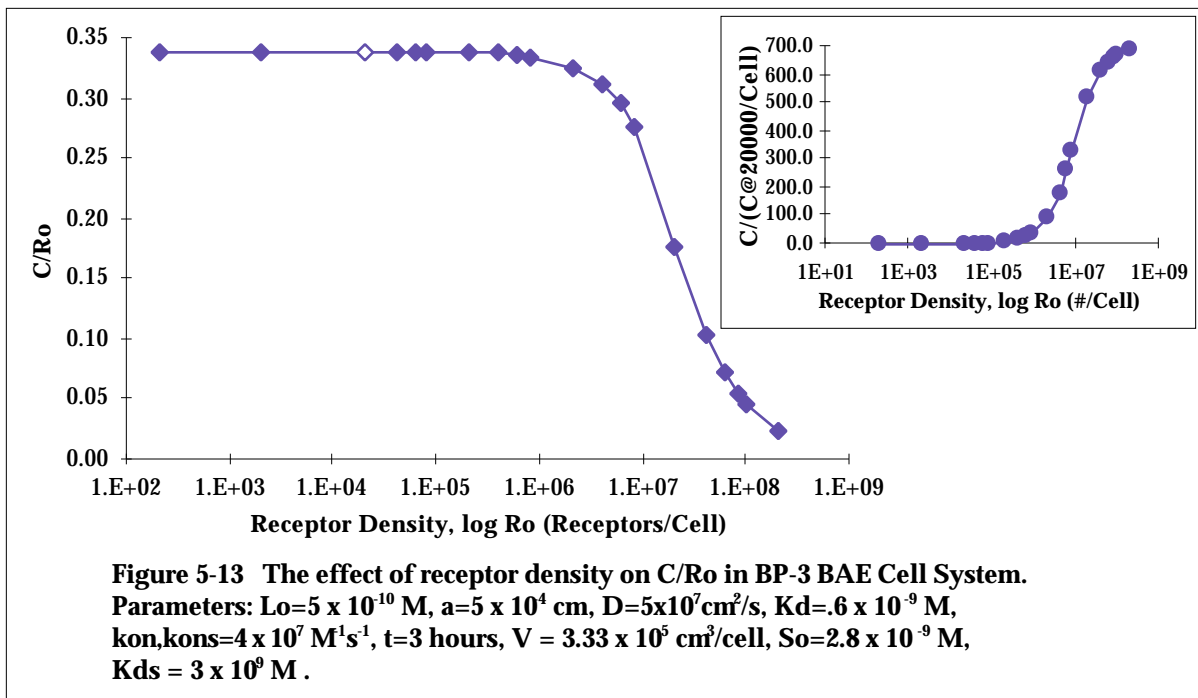
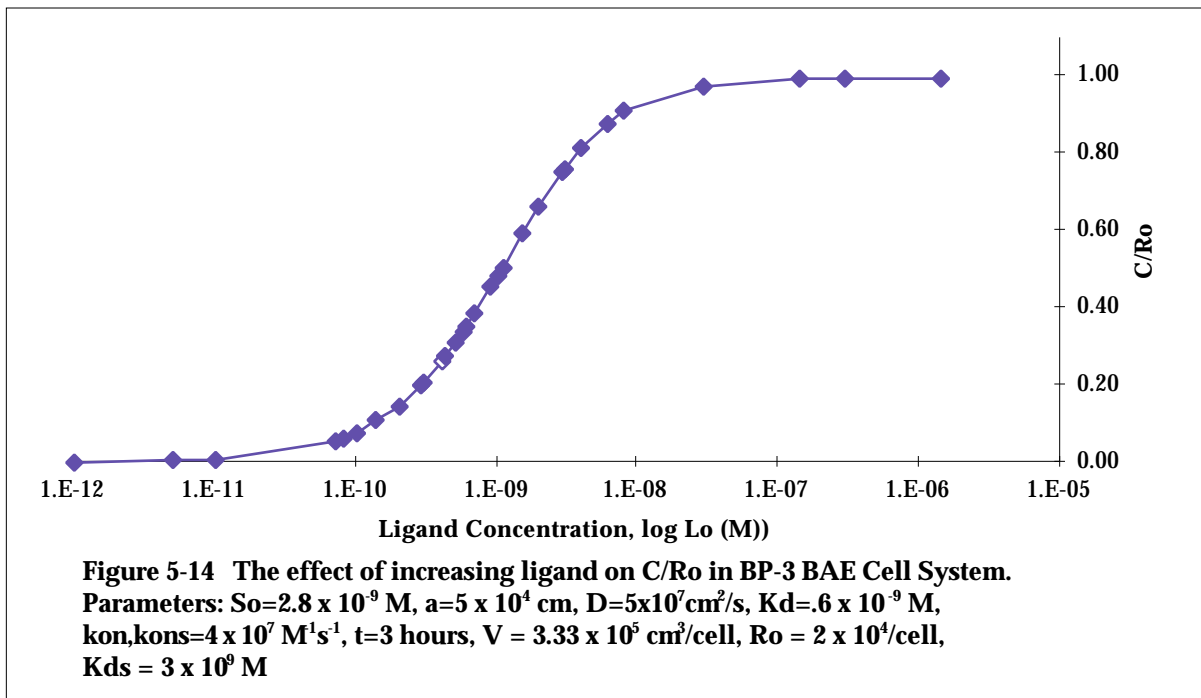


Figure 5-13 shows that as the number of available receptors on the cell surface increases from 2×10^2 - 2×10^8 receptors/cell, C/Ro decreases. The decrease in the percent of receptor occupancy begins at 2×10^6 receptors/cell. The decrease of C/Ro with increased receptor is similar to the Basic BAE Cell System Model with the same starting point of decrease, however, the maximal level of complexes is less in the IGF-I/IGFBP-3 BAE Cell System Model. It should be noted that the decrease of C/Ro as receptor density increases does not represent a decrease in surface complexes as seen with the inset of Figure 5-13. As receptor density increases, surface complexes also increase.



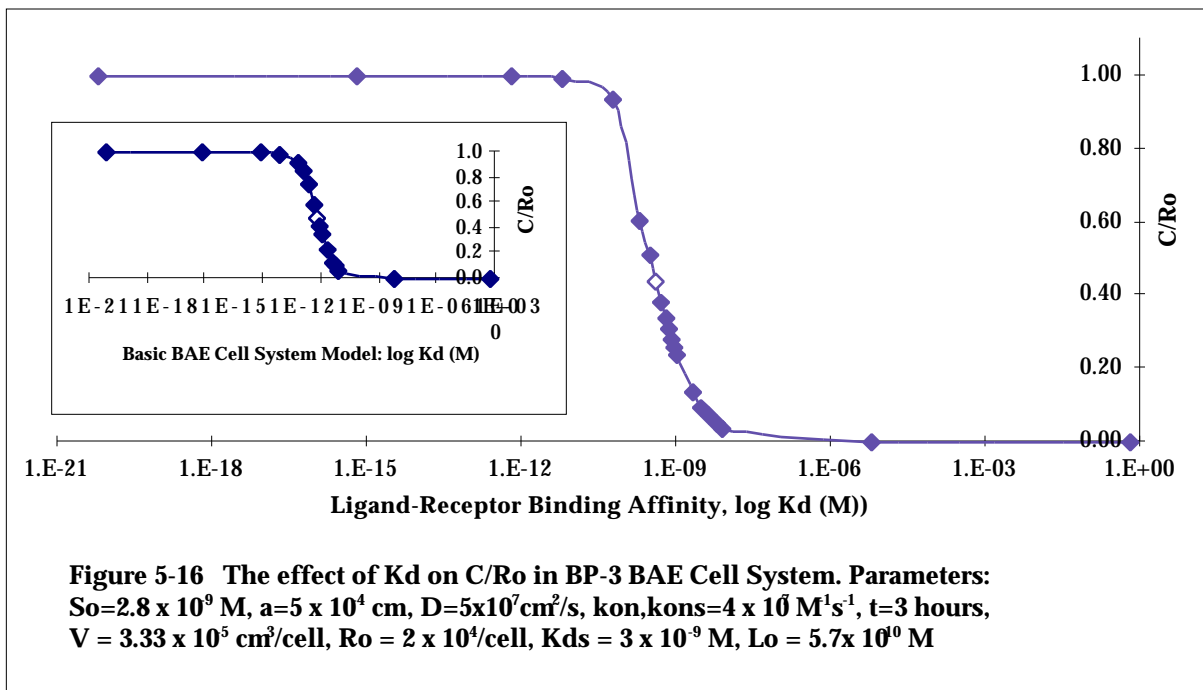
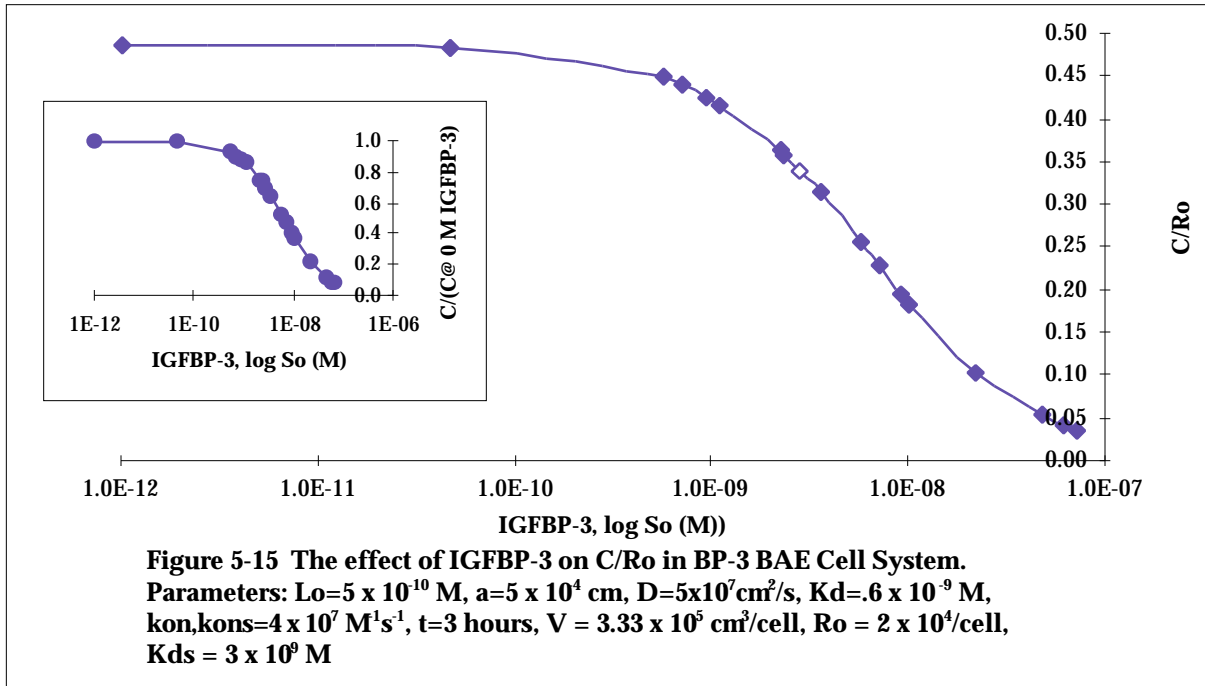
The effect of ligand concentration (L_0) on C/R_0 is presented in Figure 5-14. There are few surface complexes predicted at very low ligand concentrations (1×10^{-12} - 1×10^{-11} M). There is an increase in C/R_0 as L_0 increases from 7.1×10^{-11} M to 8×10^{-9} M with a half-maximal increase at 1×10^{-9} M. The increase levels off at molar concentrations exceeding 1.4×10^{-7} M when C/R_0 equals 1, indicating that all free receptors are bound. This also occurred with the Basic BAE Cell System Model. The Basic BAE Cell System Model increase of C/R_0 plateaus an order of magnitude faster than this model. This may be due to the presence of exogenous IGFBP-3 which forces the system to require a greater ligand concentration to reach maximal C/R_0 .



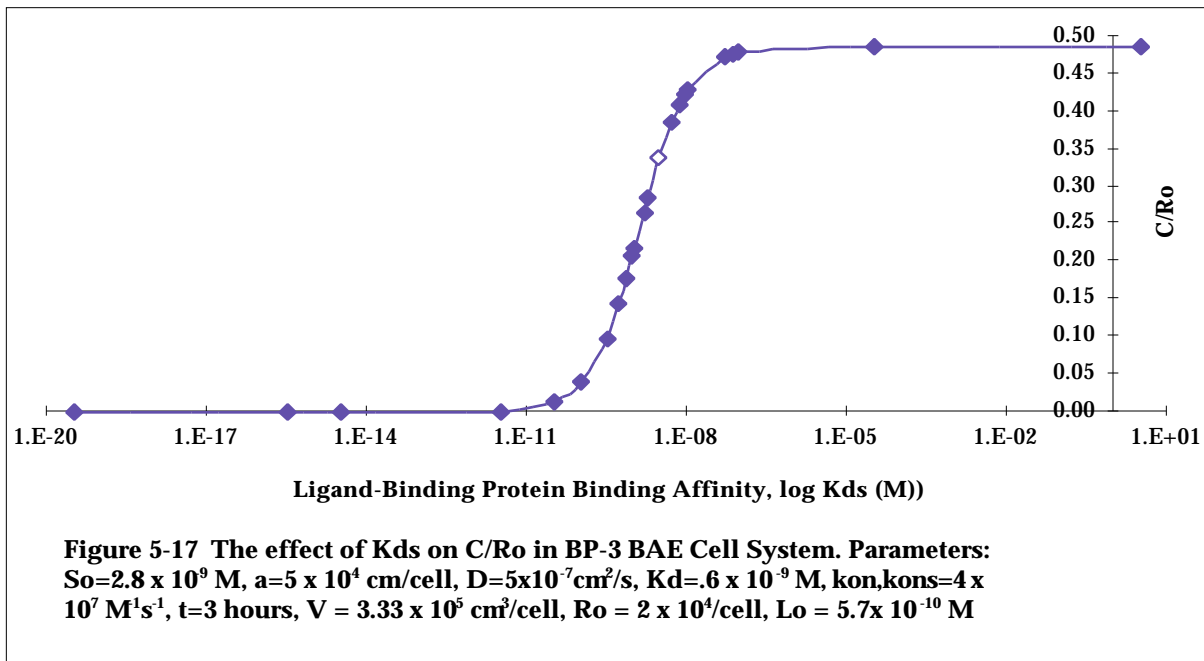
Exogenous IGFBP-3 (S_0) has a decreasing effect on C/R_0 at all values observed, (Figure 5-15). The half-maximal decrease occurs at an IGFBP-3 concentration of 5.6×10^{-9} M.

Figure 5-16 demonstrates the effect of ligand-receptor binding affinity (K_D) on C/R_0 . As K_D increases from 6×10^{-21} M to 6×10^{-16} M, no significant change can be seen in surface complexes. C/R_0 starts to decrease at 6×10^{-11} M and undergoes a steep decline at larger K_D values through 8×10^{-9} M with a half-maximal decrease at 3×10^{-10} M. A low

amount of surface complexes is predicted at K_D values of 6×10^{-6} M though .6 M. This is exactly the same response as seen with the Basic BAE Cell System Model shown in the inset of Figure 5-16.



The effect of increasing IGF-I/IGFBP-3 binding affinity, K_D^s , on C/Ro can be seen in Figure 5-17. At extremely high values of K_D^s ($3 \times 10^{-20} \text{ M} - 3 \times 10^{-12} \text{ M}$), few surface complexes are predicted. At these values, IGFBP-3 has a higher binding affinity for IGF-I than IGF-IR ($K_D = .6 \times 10^{-9} \text{ M}$) and probably will compete effectively for IGF-I. As binding affinity K_D^s decreases from $3 \times 10^{-11} \text{ M}$ to $9 \times 10^{-8} \text{ M}$, C/Ro increases significantly with a half-maximal increase at $1.5 \times 10^{-9} \text{ M}$. The increase of C/Ro levels off at $3 \times 10^{-5} \text{ M}$ and reaches essentially the same level of C/Ro as seen with the Basic BAE Cell System Model.



The ratio of K_D^s to K_D , does not affect surface complexes when low concentrations of IGFBP-3 ($0 - 1 \times 10^{-12} \text{ M}$) are present in the system. Surface complexes experience an overall decrease of C/Ro when IGFBP-3 concentrations are comparable or greater than the IGF-I present in the system, as compared to the system with low concentrations of IGFBP-3, and as K_D^s/K_D increases C/Ro increases, (Figure 5-18). This may be due to decreased free receptor availability. The inset of Figure 5-18 shows that as IGFBP-3 concentration increases, the ratio of the number of receptors to the number of IGFBP-3 decreases.

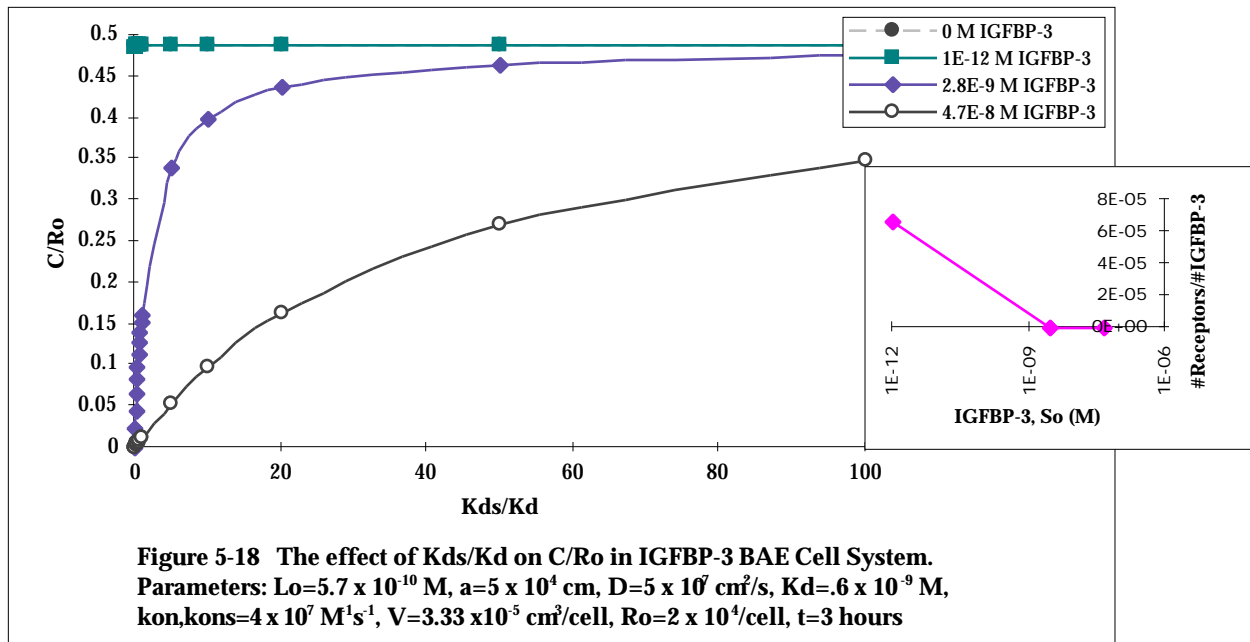
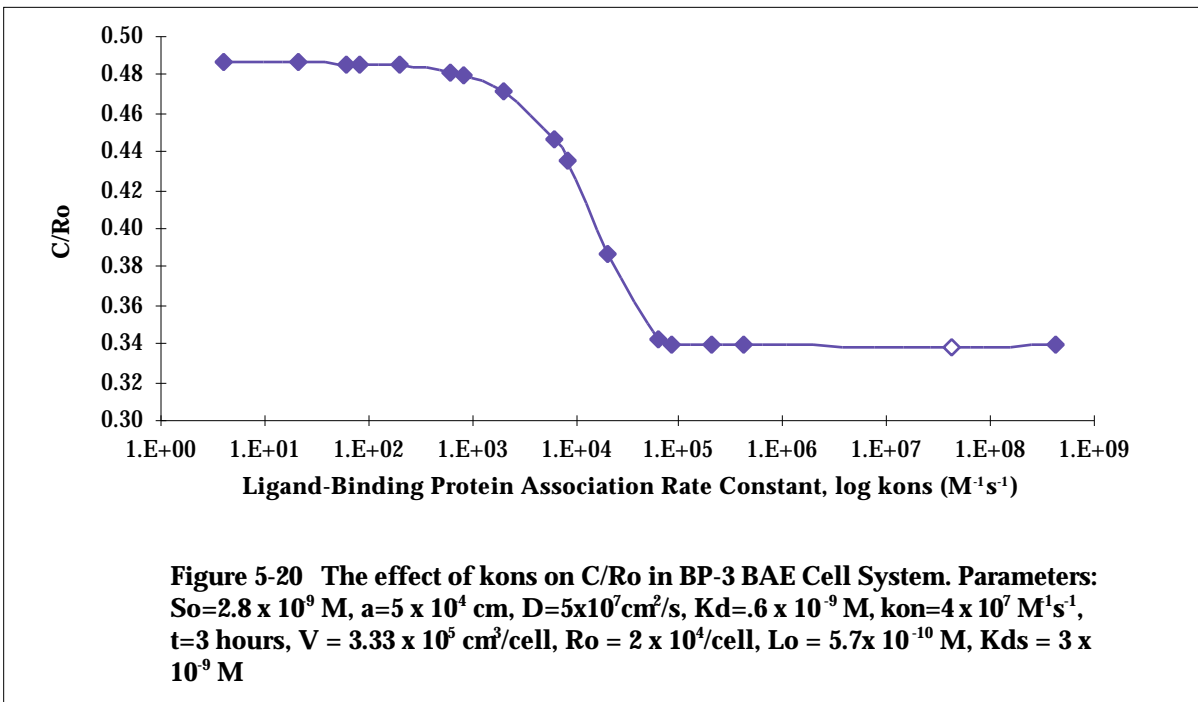
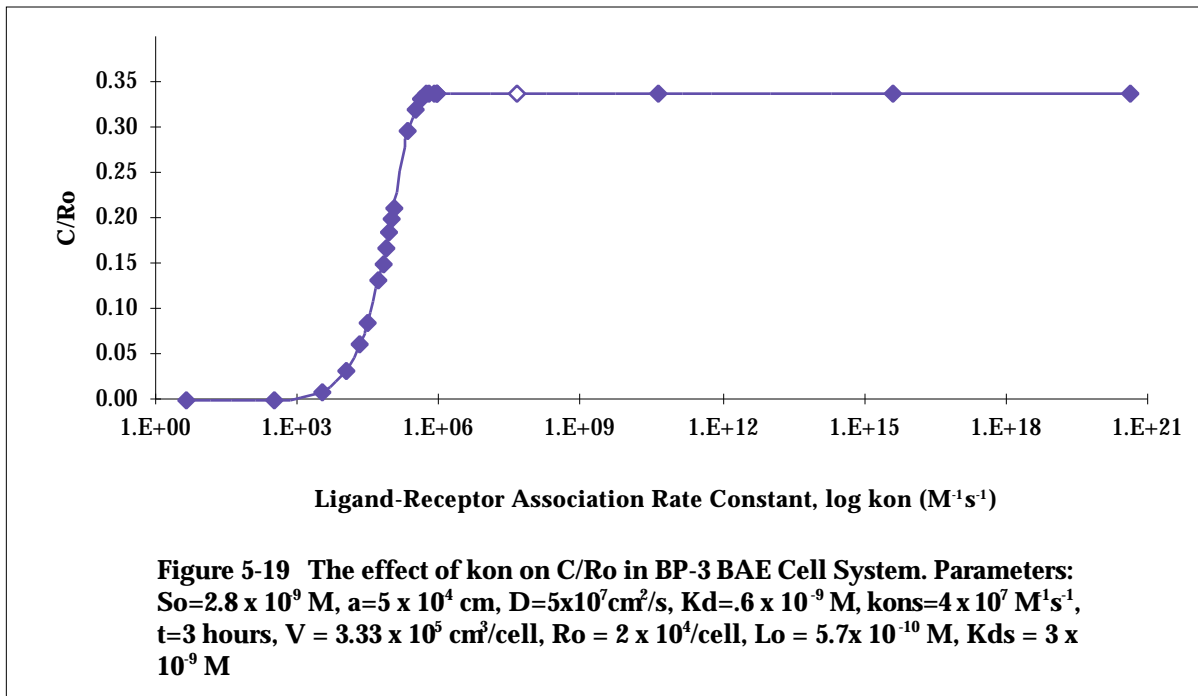


Figure 5-19 shows the variation of the association rate constant, k_{on} ($4 - 4 \times 10^{20} \text{ M}^{-1}\text{s}^{-1}$). This is the same response as seen with the Basic BAE Cell System Model with a lower maximal level of surface complexes seen with the IGF-I/IGFBP-3 BAE Cell System Model. At low values of k_{on} , C/R_0 is very low also. A low amount of surface complexes is predicted between $4 - 3 \times 10^3 \text{ M}^{-1}\text{s}^{-1}$. C/R_0 increases between $1 \times 10^4 \text{ M}^{-1}\text{s}^{-1} - 6 \times 10^5 \text{ M}^{-1}\text{s}^{-1}$ and plateaus at $7 \times 10^5 \text{ M}^{-1}\text{s}^{-1}$. The half maximal increase for this system is the same as for the Basic BAE Cell system Model and occurs at $6 \times 10^4 \text{ M}^{-1}\text{s}^{-1}$. However, this system greater association rate constant to show an increase and final plateau of C/R_0 .

The effect of increasing the IGF-I/IGFBP-3 association rate constant, k_{on} , can be seen in Figure 5-20. There is no decrease in surface complexes when ligand-soluble receptor association rate constants are very low ($4 - 8 \times 10^2 \text{ M}^{-1}\text{s}^{-1}$). As k_{on} increases from $2 \times 10^3 \text{ M}^{-1}\text{s}^{-1}$ to $2 \times 10^4 \text{ M}^{-1}\text{s}^{-1}$, C/R_0 decreases slightly. The half maximal increase occurs at $2 \times 10^4 \text{ M}^{-1}\text{s}^{-1}$. The decreasing effect levels out at $6 \times 10^4 \text{ M}^{-1}\text{s}^{-1}$. The IGF-I/IGFBP-3 association rate constant effect on C/R_0 is exactly opposite of the effect of the IGF-I/IGF-IR association rate constant on C/R_0 .



The IGF-I/IGFBP-3 BAE Cell System Model predicts that IGFBP-3 acts as a competitor for IGF-I in regard to IGF-I/IGF-IR binding. The increase in receptor density, R_o , IGFBP-3 concentration, S_o , the equilibrium constant, K_D , and the IGF-I/IGFBP-3 association rate constant, k_{on}^s , results in a decrease of ligand-receptor surface complexes. As mentioned previously, a decrease in C/R_o in response to varying a system parameter usually represents a decrease in surface complexes with the exception of varying receptor density. An increase in ligand concentration, L_o , IGF-I/IGFBP-3 binding affinity, K_d^s , and the ligand-receptor association rate constant, k_{on} , results in an increase of ligand-receptor surface complexes. As with the Basic BAE Cell System Model, down-regulation of cell surface receptors is not accounted for in the model and could affect the increase in C/R_o . This system requires a larger parameter values to reach a maximal C/R_o than the Basic BAE Cell System Model. This is likely due to competition for ligand binding between surface and soluble receptors. An increase in K_D^s/K_D results in an increase in surface complexes at comparable or greater concentrations of IGFBP-3, as compared to IGF-I, present in the system. Surface complexes were unaffected by increasing K_D^s/K_D when low concentrations of IGFBP-3 are present. The system reaches steady state in seven minutes.

IGF-I/p9 HS BAE Cell System Model:

The IGF-I/p9 HS BAE Cell System Model is the same as the IGF-I/IGFBP-3 BAE Cell System Model except it includes parameters for IGF-I/p9 HS binding and not the IGF-I/IGFBP-3 binding parameters previously used. This model is based on IGF-I/IGF-IR binding and IGF-I/p9 HS binding, (Figure 5-21).

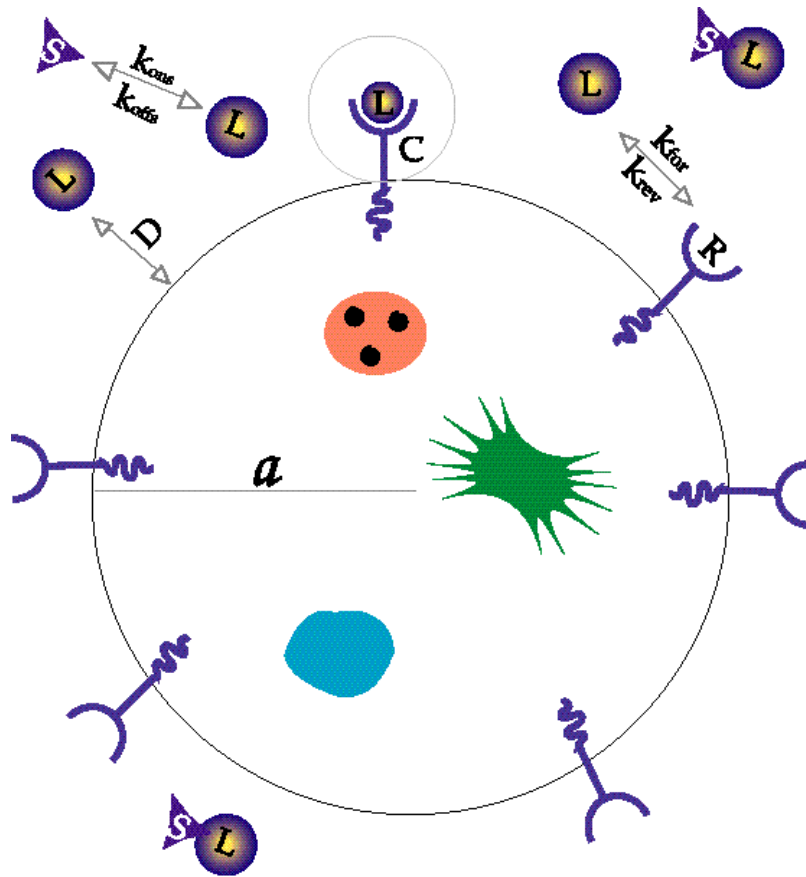


Figure 5-21 Schematic illustration of IGF-I/p9 HS BAE Cell System Model. All variables and parameters shown on the model are described by symbol in the text.

The transient expressions for the model are presented in Table 5-6. The expressions are the same as the IGF-I/IGFBP-3 BAE Cell System Model with p9 HS replacing IGFBP-3 as the soluble receptor.

Table 5-6 IGF-I/p9 HS BAE Cell System Model Equations
$dR/dt = -k_{for}[L][R] + k_{rev}[C]$
$dC/dt = k_{for}[L][R] - k_{rev}[C]$
$V(dL/dt) = -k_{for}[L][R] + k_{rev}[C] - V k_{on}^s[L][S] + V k_{off}^s[X]$
$V(dS/dt) = -V k_{on}^s[L][S] + V k_{off}^s[X]$
$V(dX/dt) = V k_{on}^s[L][S] - V k_{off}^s[X]$
where $k_{for} = k_{on}/(1+(k_{on}R/4 aD))$ and $k_{rev} = k_{off}/(1+(k_{on}R/4 aD))$

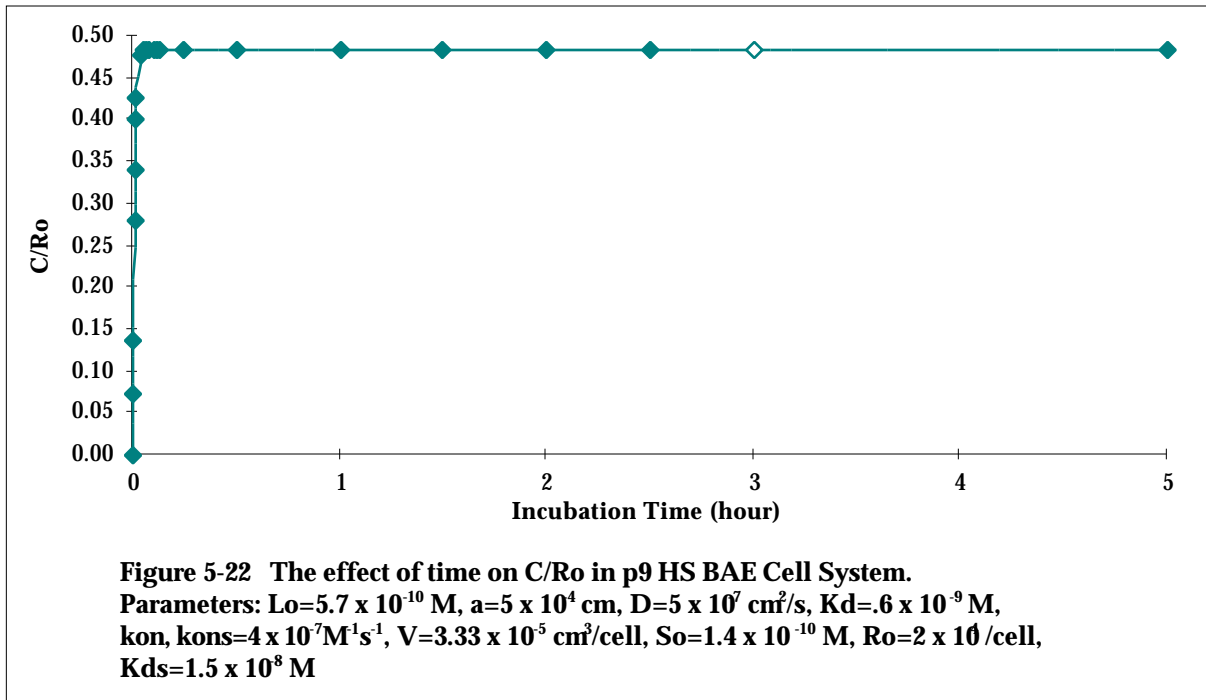
System values and parameters and initial conditions for the IGF-I/p9 HS BAE Cell System Model are shown in Table 5-7. The association rate constant (k_{on}) for IGF-I/IGF-IR binding was varied and the dissociation rate constant (k_{off}) for IGF-I/IGF-IR binding was determined as a function of k_{on} and K_d . The association rate constant (k_{on}^s) for IGF-I/p9 HS binding was varied and the dissociation rate constant (k_{off}^s) for IGF-I/p9 HS binding was determined as a function of k_{on}^s and K_d^s .

The FORTRAN program used for the IGF-I/p9 HS BAE Cell System Model can be found in Appendix B. Results for the IGF-I/p9 HS BAE Cell System Model are presented as a ratio of the ligand-receptor cell surface complexes (C) to the initial unbound receptors (Ro) as C/Ro. Most results are presented on a log scale. Base system parameters are denoted by an open diamond.

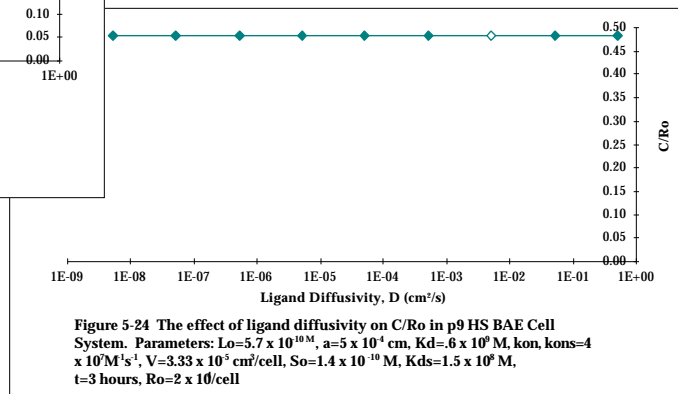
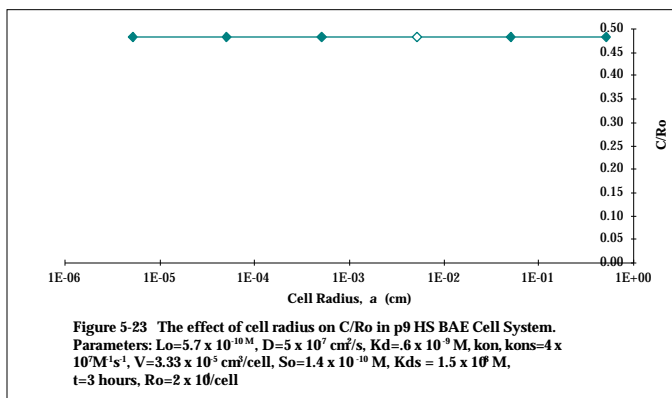
Table 5-7 IGF-I/p9 HS BAE Cell System Model Parameters and Initial Conditions

<i>Parameter Values</i>		
K_D	$.6 \times 10^{-9} \text{ M}$	Jones and Clemmons, 1995
k_{on}	$4 \times 10^7 \text{ M}^{-1}\text{s}^{-1}$	Forsten and Lauffenberger, 1992
K_D^s	$1.5 \times 10^{-8} \text{ M}$	Experimental
k_{on}^s	$4 \times 10^7 \text{ M}^{-1}\text{s}^{-1}$	Forsten and Lauffenberger, 1992
R_o	$2 \times 10^4 \text{ receptors/cell}$	Forsten and Lauffenberger, 1992
a	$5 \times 10^{-4} \text{ cm}$	Forsten and Lauffenberger, 1992
D	$5 \times 10^{-7} \text{ cm}^2/\text{s}$	Geankopolis, 1993
V	$3.33 \times 10^{-5} \text{ cm}^3/\# \text{ of cells}$	Experimental
L_o	$5.7 \times 10^{-10} \text{ M}$	Experimental
S_o	$1.4 \times 10^{-10} \text{ M}$	Experimental
<i>Initial Conditions</i>		
R/R_o	1.0	all receptors initially unbound
C/R_o	0.0	no initial complexes
L/K_D	L_o/K_D	
S/S_o	1.0	homogeneously distributed soluble receptors
X/S_o	0.0	no initial complexes

Initial analysis of the IGF-I/p9 HS BAE Cell System Model was performed over a range of time periods from 0-5 hours. (Figure 5-22) The system reaches steady state in seven minutes. This is not seen experimentally which may be due to neglected cell system effects such as possible p9 HS cell surface binding, p9 HS secretion and IGF-I and IGF-IR secretion and degradation.



The remainder of the IGF-I/p9 HS BAE Cell System Model analysis was done at a steady state time period of 3 hours, initial ligand concentration (L_0) of 5.7×10^{-10} M and p9 HS concentration (S_0) of 1.4×10^{-10} M. These parameter values were used to mimic experimental binding studies, (See Section 2.J). This system is also insensitive to cell radius and ligand diffusivity, (Figure 5-23, Figure 5-24).



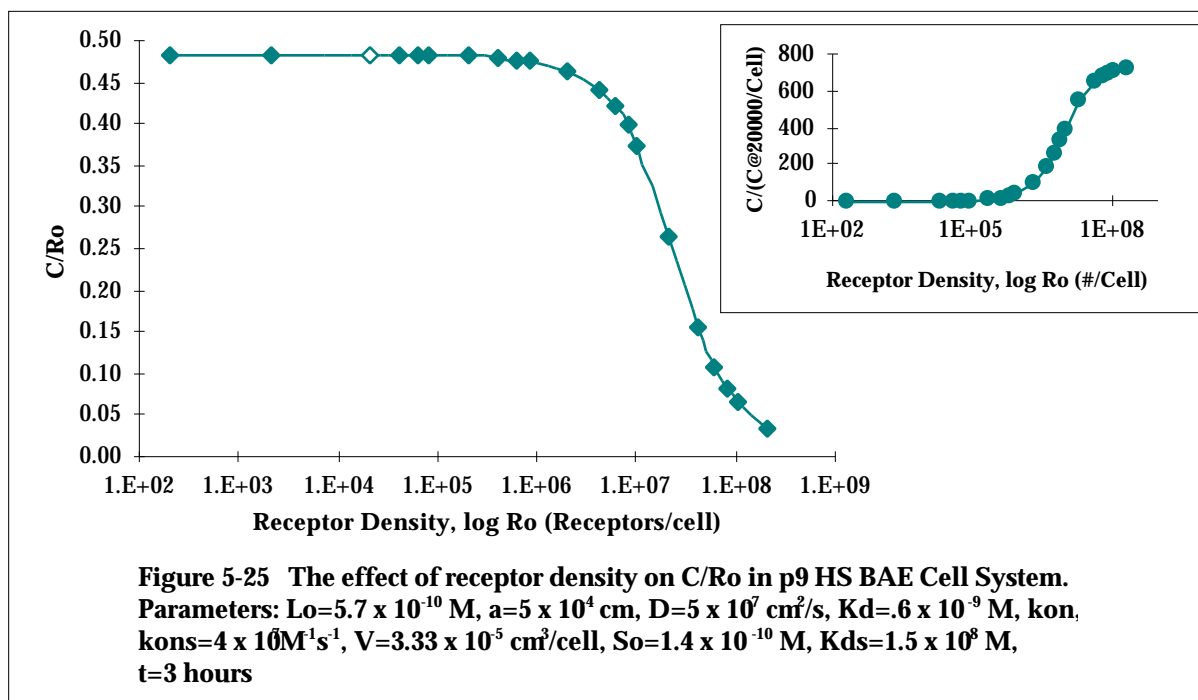
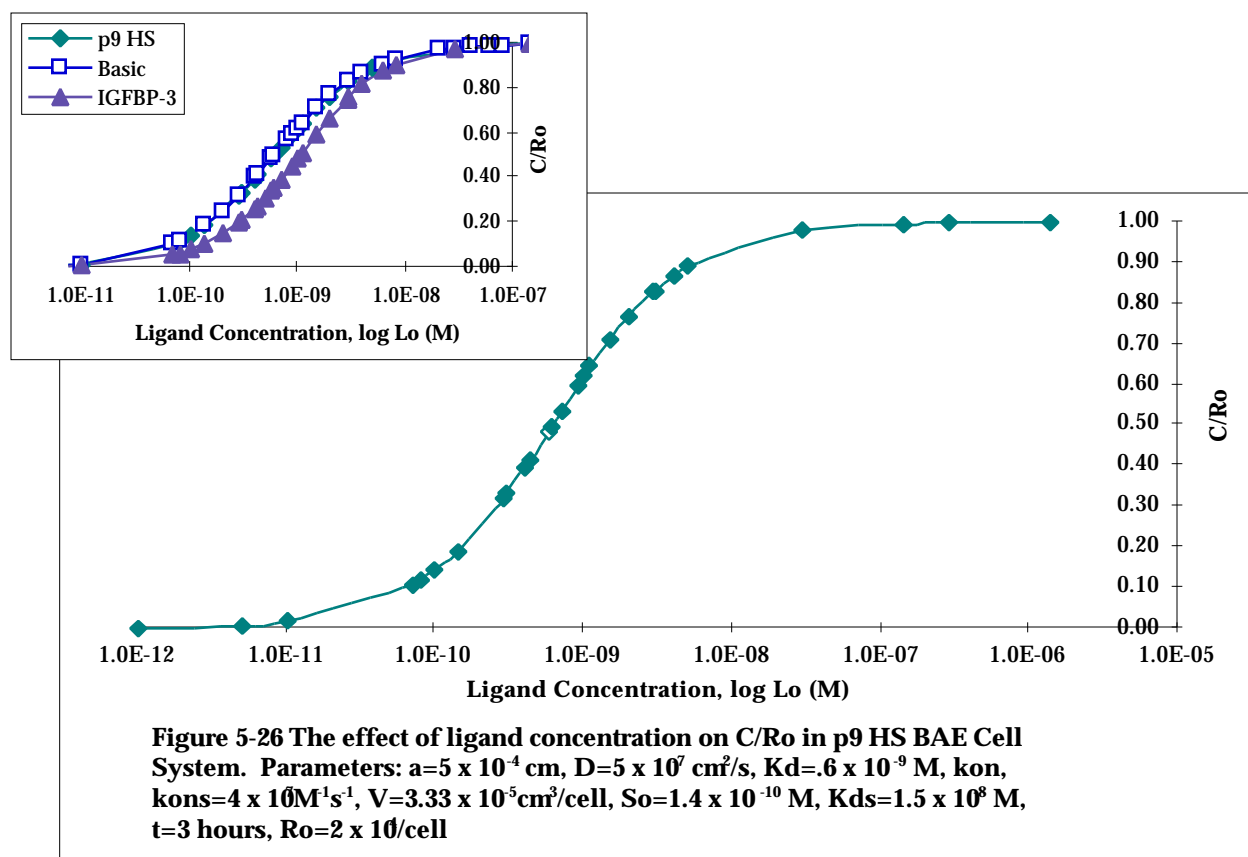


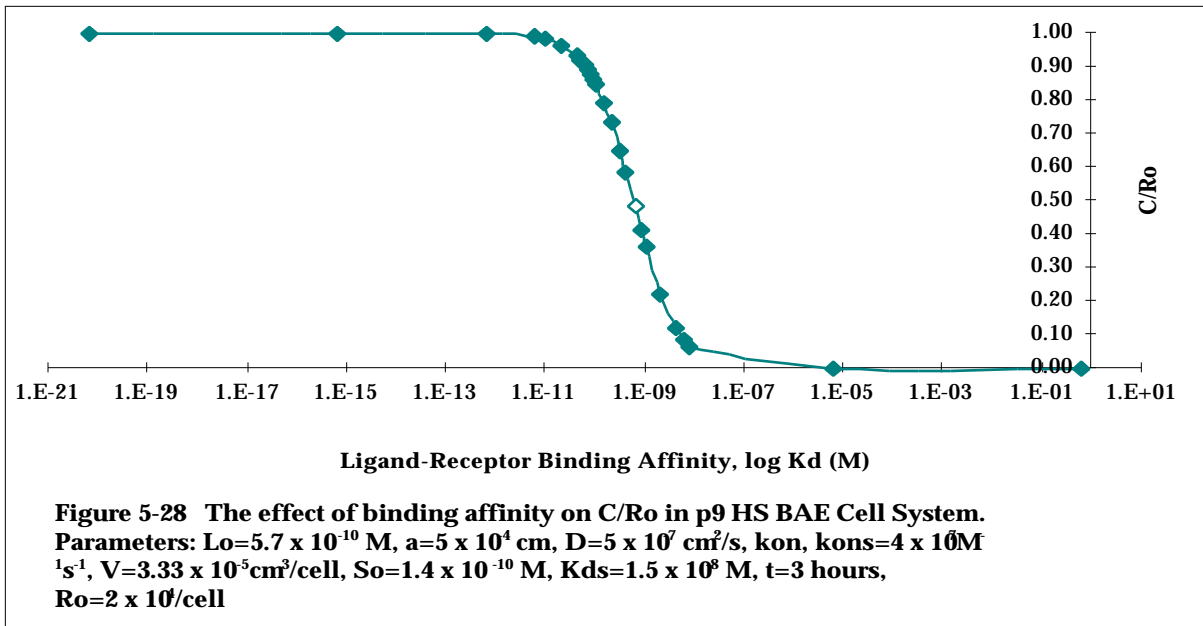
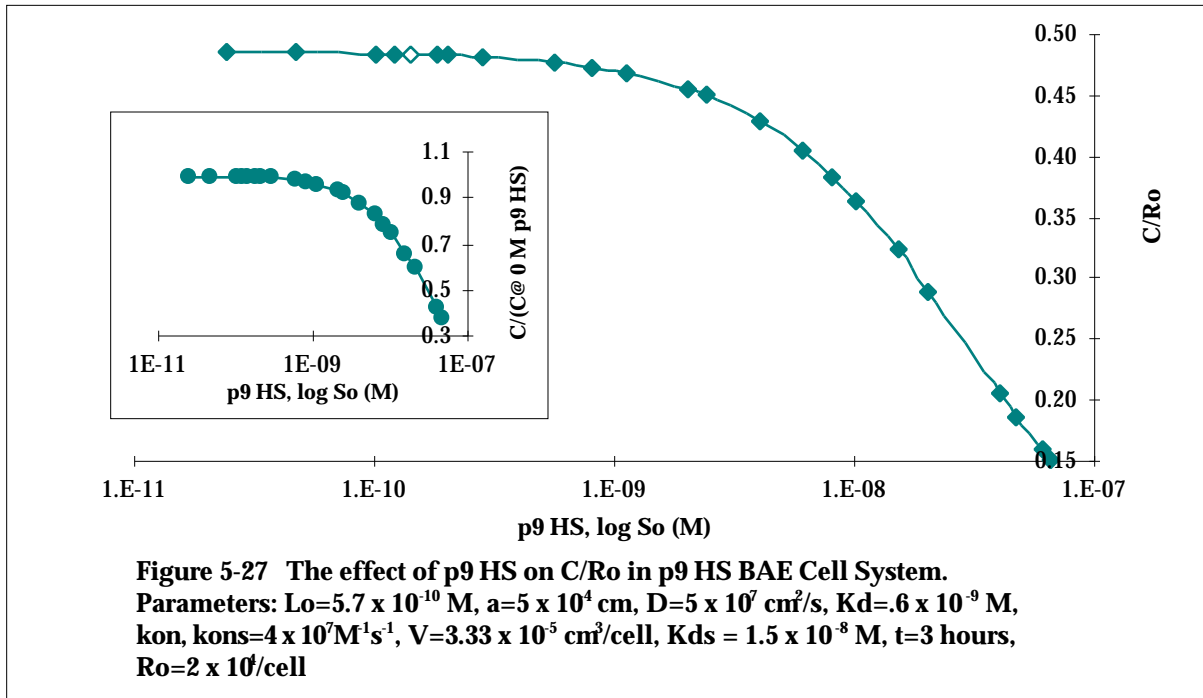
Figure 5-25 shows that as the number of available receptors on the cell surface increases from 2×10^2 - 2×10^8 receptors/cell, C/Ro decreases. The decrease in surface complexes begins at 2×10^6 receptors/cell. The decrease in C/Ro as receptor increases does not represent a decrease in actual surface complexes as seen with the inset of Figure 5-25. The decreasing effect of receptor density on ligand-receptor surface complexes is similar to the Basic and IGF-I/IGFBP-3 BAE Cell System Models.

The effect of ligand concentration (L_0) on C/Ro is presented in Figure 5-26. There are few surface complexes predicted at very low ligand concentrations. (1×10^{-12} M - 5×10^{-12} M) with an increase in C/Ro as L_0 increases from 1×10^{-11} M to 2.9×10^{-8} M. A half maximal increase occurs at 6×10^{-10} M. The increase begins to level off at p9 HS concentrations exceeding 1.4×10^{-7} M. This system reaches the maximal value of C/Ro at the same ligand concentration as the Basic BAE Cell System Model. The IGF-I/IGFBP-3 Cell System Model required slightly more ligand to reach maximal C/Ro. This suggest that p9 HS is not as potent of a competing soluble receptor as IGFBP-3 which is reflected in the lower binding affinity of p9 HS. The similarities in the response of surface complexes in all three models may suggest that the ligand concentration is more important to IGF-I/IGF-IR binding than the presence of IGFBP-3 or p9 HS.



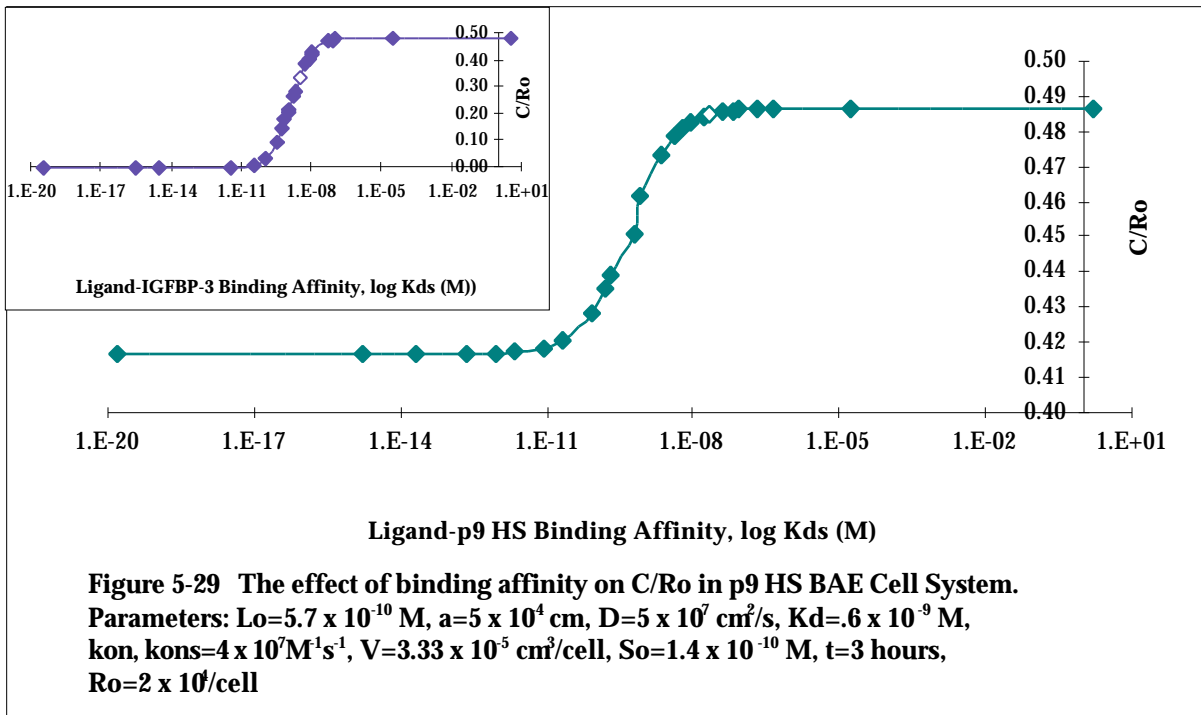
Exogenous p9 HS does not affect C/Ro until p9 HS is present at high concentrations (5.6×10^{-10} M - 6.5×10^{-8} M) where surface complexes are slightly inhibited. Increasing p9 HS concentration, as a soluble receptor in the system, has less of a decreasing effect on C/Ro than IGFBP-3, as a soluble receptor, which may be due to the higher binding affinity of IGFBP-3 and IGF-I than p9 HS and IGF-I, (Figure 5-27). There is, however, no increase in overall C/Ro with the addition of p9 HS as compared to the IGF-I/IGFBP-3 BAE Cell System Model.

Figure 5-28 demonstrates the effect of ligand-receptor binding affinity (K_D) on C/Ro. As K_D increases from 6×10^{-21} M to 1×10^{-11} M, no decrease of surface complexes is predicted. C/Ro starts to decrease at 2×10^{-11} M and continues through 6×10^{-10} M with a half maximal decrease occurring at 6×10^{-10} M. A low amount of surface complexes is predicted when K_D falls below 6×10^{-6} M. This is a similar trend to the Basic and IGFBP-3 BAE Cell System Models.



The effect of increasing IGF-I/p9 HS binding affinity, K_D^s , on C/Ro can be seen in Figure 5-29. As the binding affinity decreases from 2×10^{-11} M to 4×10^{-9} M, C/Ro increases slightly with a half maximal increase occurring at 6×10^{-10} M. The increase of C/Ro levels off at 6×10^{-5} M. The IGF-I/IGFBP-3 BAE Cell System Model predicted a

larger increase of C/Ro with decreased IGF-I/IGFBP-3 binding affinity. The IGF-I/p9 HS BAE Cell System Model is less sensitive to K_d^s than the IGF-I/IGFBP-3 BAE Cell System Model.



Increasing the ratio of K_D^s to K_D^r , has little effect on C/Ro for p9 HS concentration similar or less than the IGF-I in the system. Surface complexes experience an overall decrease of C/Ro when p9 HS concentrations are much greater than the IGF-I present in the system, as compared to the system when low concentrations of p9 HS are present. As K_D^s/K_D^r increases with high concentrations of p9 HS present in the system, C/Ro increases, (Figure 5-30). The IGF-I/p9 HS BAE Cell System Model requires a higher concentration of soluble receptor (p9 HS) than the IGF-I/IGFBP-3 BAE Cell System Model requires to result in an overall decrease of C/Ro and an increasing trend with increasing K_D^s/K_D^r .

Figure 5-31 shows the variation of the IGF-I/IGF-IR association rate constant, k_{on} ($4 - 4 \times 10^{20}$ M⁻¹s⁻¹). This is the same response seen with increasing k_{on} for the Basic and IGFBP-3 BAE Cell System Models. At low values of k_{on} , C/Ro is very low also. C/Ro eventually plateaus at 4×10^5 M⁻¹s⁻¹.

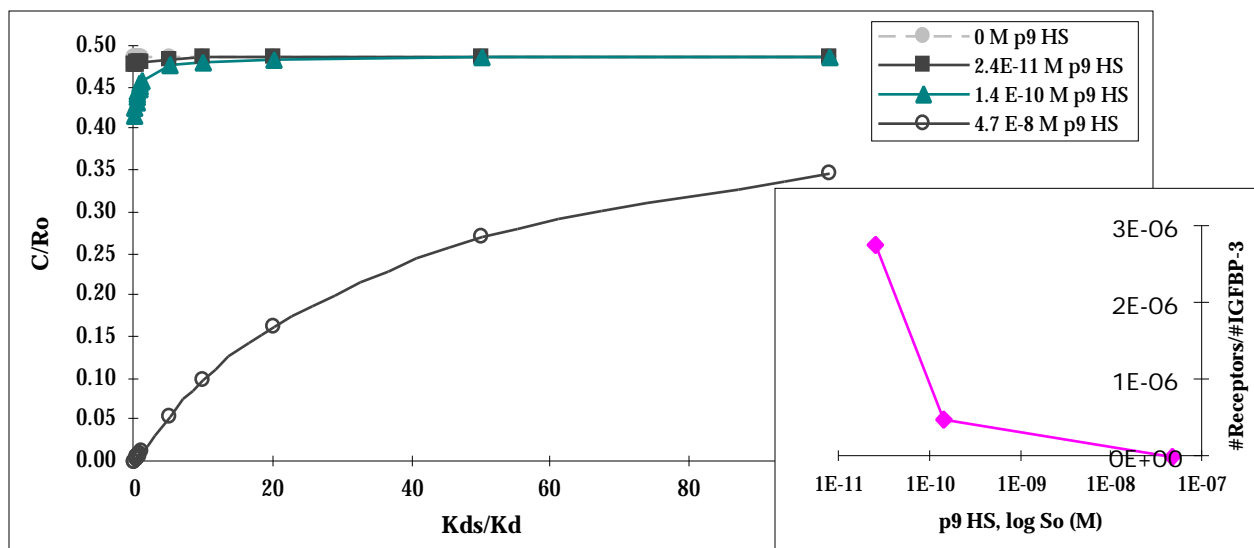


Figure 5-30 The effect of Kds/Kd on C/Ro in p9 HS BAE Cell System.
Parameters: $L_0=5.7 \times 10^{-10} \text{ M}$, $a=5 \times 10^4 \text{ cm}$, $D = 5 \times 10^7 \text{ cm}^2/\text{s}$, $K_d=.6 \times 10^{-9} \text{ M}$,
 $k_{on}, k_{ons}=4 \times 10^7 \text{ M}^{-1} \text{ s}^{-1}$, $V=3.33 \times 10^5 \text{ cm}^3/\text{cell}$, $S_0=1.4 \times 10^{-10} \text{ M}$, $t=3 \text{ hours}$, $R_0=2 \times 10^4/\text{cell}$

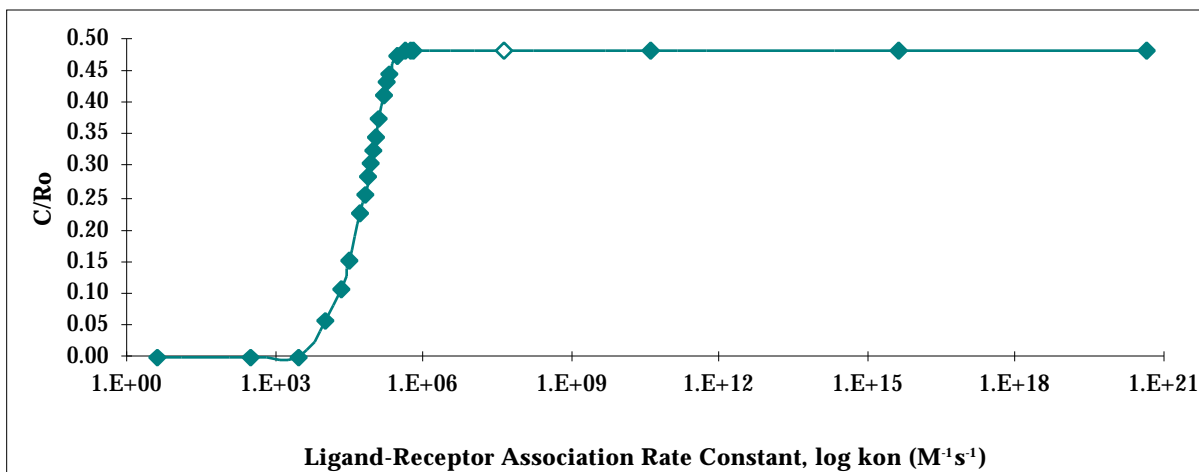
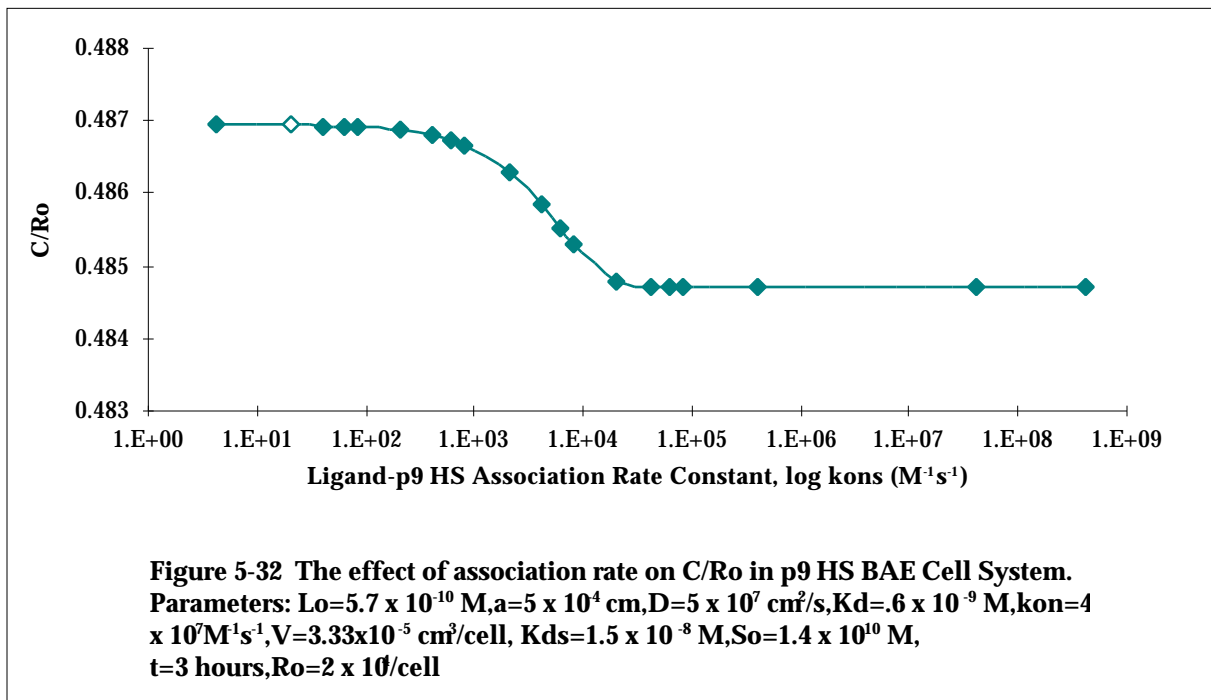


Figure 5-31 The effect of association rate on C/Ro in p9 HS BAE Cell System.
Parameters: $L_0=5.7 \times 10^{-10} \text{ M}$, $a=5 \times 10^4 \text{ cm}$, $D=5 \times 10^7 \text{ cm}^2/\text{s}$, $K_d=.6 \times 10^{-9} \text{ M}$,
 $k_{ons}=4 \times 10^7 \text{ M}^{-1} \text{ s}^{-1}$, $V=3.33 \times 10^5 \text{ cm}^3/\text{cell}$, $K_{ds}=1.5 \times 10^{-8} \text{ M}$, $S_0=1.4 \times 10^{-10} \text{ M}$,
 $t=3 \text{ hours}$, $R_0=2 \times 10^4/\text{cell}$

The effect of increasing the IGF-I/p9 HS association rate constant, k_{on} , on C/Ro can be seen in Figure 5-32. As k_{on} increases from $4 \text{ M}^{-1}\text{s}^{-1}$ to $4 \times 10^8 \text{ M}^{-1}\text{s}^{-1}$, C/Ro decreases slightly. The decreasing trend for C/Ro is similar to the IGF-I/IGFBP-3 BAE Cell System Model but differs in that the decrease predicted with the IGF-I/p9 HS BAE Cell System Model as k_{on} increases is much less substantial than seen with the IGF-I/IGFBP-3 BAE Cell System Model. This may be to the lower concentration of p9 HS present in this system. IGFBP-3 concentration in the IGF-I/IGFBP-3 BAE Cell System Model is an order of magnitude higher than the p9 HS concentration used in this model. The binding affinity for p9 HS and IGF-I is also less than the binding affinity for IGF-I and IGFBP-3.



The IGF-I/p9 HS BAE Cell System Model predicts that p9 HS behaves as a competitor for IGF-I/IGF-IR binding; however, p9 HS is not as effective of a competitor as IGFBP-3 as seen in the comparison of all three models. The increase in receptor density, R_0 , and IGF-I/IGF-IR equilibrium constant, K_D , results in a decrease of C/R_0 . An increase in ligand concentration, L_0 , IGF-I/p9 HS binding affinity, K_D^s , and the ligand-receptor association rate constant, k_{on} , results in an increase of C/R_0 . An increase in K_D^s/K_D results in an increase in surface complexes at high concentrations of p9 HS present in the system. Surface complexes were unaffected by increasing K_D^s/K_D when low concentrations of p9 HS are present. An increase in p9 HS concentration, S_0 , only decreases C/R_0 at the highest molar concentrations examined. An increase of the IGF-I/p9 HS association rate constant, k_{on}^s , results in only a slight decrease of C/R_0 . The differences in this model as compared to the IGF-I/IGFBP-3 BAE Cell System Model may be due to concentration differences between the two models. The concentration of p9 HS for this model is an order of magnitude less than IGFBP-3 in the previous system. The binding affinity for p9 HS and IGF-I (1.5×10^{-8} M) is less than the binding affinity of IGFBP-3 and IGF-I (3×10^{-9} M). The system reaches steady state in seven minutes.

Complex BAE Cell System Model:

The Complex BAE Cell System Model is a more complicated version of the IGF-I/IGFBP-3 and IGF-I/p9 HS BAE Cell System Models due to the simultaneous addition of both soluble receptors IGFBP-3 and p9 HS into the system. This model is based on IGF-I/IGF-IR binding, IGF-I/IGFBP-3 and IGF-I/p9 HS binding, (Figure 5-33).

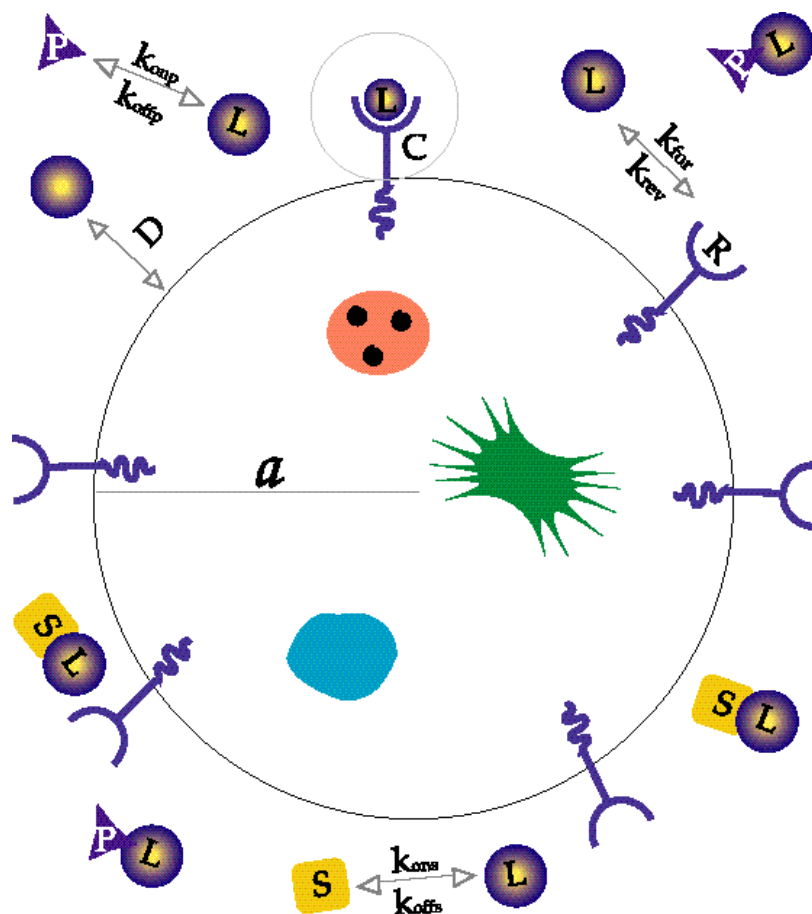


Figure 5-33 Schematic illustration of Complex BAE Cell System Model. All variables and parameters shown on the model are described by symbol in the text.

The transient expressions for the model are presented in Table 5-8. The expressions are similar to the IGF-I/IGFBP-3 and IGF-I/p9 HS BAE Cell System Models with the inclusion of both IGFBP-3 and p9 HS as soluble receptors. The change in free ligand concentration becomes a more complicated expression with dual soluble receptors. Two additional time derivatives are added to the system to represent the change in bound and unbound soluble p9 HS, P and Q respectively. The association and dissociation

rates for IGF-I and p9 HS are k_{on}^p and k_{off}^p , respectively. The change in unbound and bound IGFBP-3 will remain as S and X , respectively as shown in Equations 6 and 7. The additional equations and the change in the existing free ligand concentration equation are as follows:

$$VdP/dt = -k_{on}^p[L][P] + k_{off}^p[Q], \quad (6)$$

$$VdQ/dt = k_{on}^p[L][P] - k_{off}^p[Q], \quad (7)$$

$$VdL/dt = -k_{for}^s[L][R] + k_{rev}^s[C] - k_{on}^s[L][S] + k_{off}^s[X] - k_{on}^p[L][P] + k_{off}^p[Q] \quad (8)$$

with k_{for}^s and k_{rev}^s as shown previously in Equation 4 and Equation 5. No binding of IGFBP-3 or p9 HS with IGF-IR, or any other cellular surface component is included. Binding between p9 HS and IGFBP-3 is neglected.

Table 5-8 Complex BAE Cell System Model Equations
$dR/dt = -k_{for}^s[L][R] + k_{rev}^s[C]$
$dC/dt = k_{for}^s[L][R] - k_{rev}^s[C]$
$V(dL/dt) = -k_{for}^s[L][R] + k_{rev}^s[C] - V k_{on}^s[L][S] + V k_{off}^s[X] - V k_{on}^p[L][P] + V k_{off}^p[Q]$
$V(dS/dt) = -V k_{on}^s[L][S] + V k_{off}^s[X]$
$V(dX/dt) = V k_{on}^s[L][S] - V k_{off}^s[X]$
$V(dP/dt) = -V k_{on}^p[L][P] + V k_{off}^p[Q]$
$V(dQ/dt) = V k_{on}^p[L][P] - V k_{off}^p[Q]$
where $k_{for}^s = k_{on}^s / (1 + (k_{on}^R / 4 aD))$ and $k_{rev}^s = k_{off}^s / (1 + (k_{on}^R / 4 aD))$

Table 5-9 Complex BAE Cell System Model Parameters and Initial Conditions

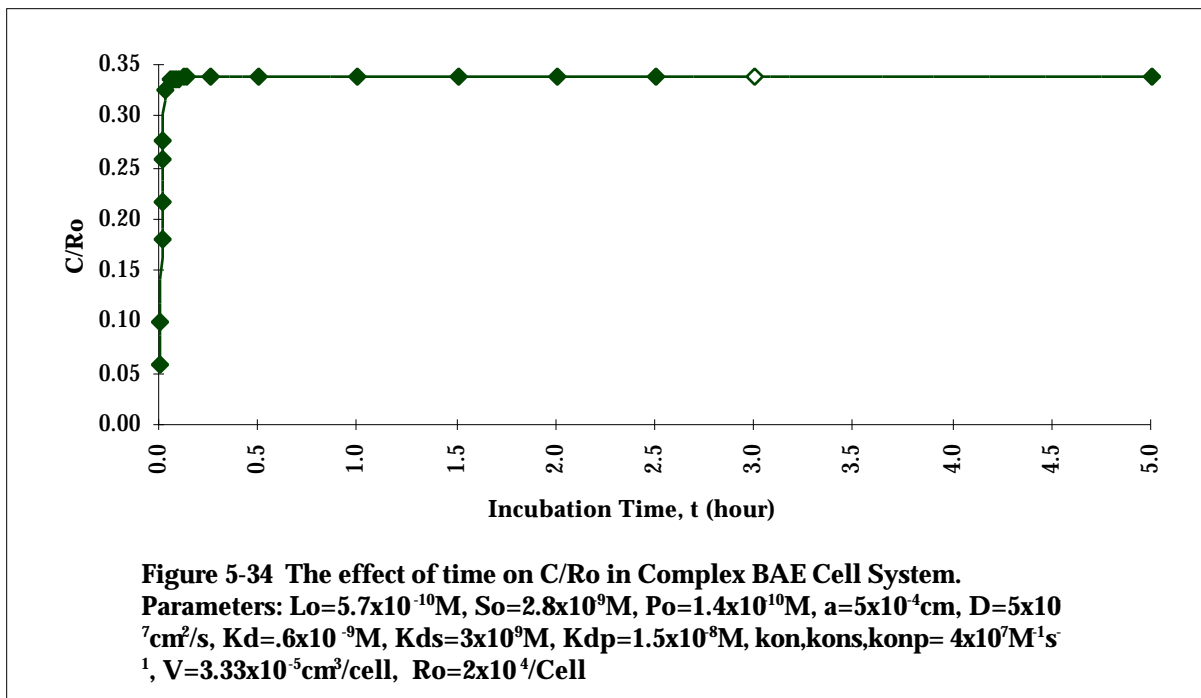
Parameter Values		
K_d	$.6 \times 10^{-9} \text{ M}$	Jones and Clemmons, 1995
k_{on}	$4 \times 10^7 \text{ M}^{-1}\text{s}^{-1}$	Forsten and Lauffenberger, 1992
K_D^s	$3 \times 10^{-9} \text{ M}$	Experimental
k_{on}^s	$4 \times 10^7 \text{ M}^{-1}\text{s}^{-1}$	Forsten and Lauffenberger, 1992
K_D^p	$1.5 \times 10^{-8} \text{ M}$	Experimental
k_{on}^p	$4 \times 10^7 \text{ M}^{-1}\text{s}^{-1}$	Forsten and Lauffenberger, 1992
R_o	$2 \times 10^4 \text{ receptors/cell}$	Forsten and Lauffenberger, 1992
a	$5 \times 10^{-4} \text{ cm}$	Forsten and Lauffenberger, 1992
D	$5 \times 10^{-7} \text{ cm}^2/\text{s}$	Geankopolis, 1993
V	$3.33 \times 10^{-5} \text{ cm}^3/\# \text{ of cells}$	Experimental
L_o	$5.7 \times 10^{-10} \text{ M}$	Experimental
S_o	$2.8 \times 10^{-9} \text{ M}$	Experimental
P_o	$1.4 \times 10^{-10} \text{ M}$	
<i>Initial Conditions</i>		
R/R_o	1.0	all receptors initially unbound
C/R_o	0.0	no initial complexes
L/K_D	L_o/K_D	
S/S_o	1.0	homogeneously distributed soluble receptors
X/S_o	0.0	no initial complexes
P/P_o	1.0	homogeneously distributed soluble receptors
Q/P_o	0.0	no initial complexes

System values and parameters and initial conditions are shown in Table 5-9. The association rate constant (k_{on}) for IGF-I/IGF-IR binding was varied and the dissociation rate constant (k_{off}) for IGF-I/IGF-IR binding was determined as a function of k_{on} and K_D . The association rate constant (k_{on}^s) for IGF-I/IGFBP-3 binding was varied and the

dissociation rate constant (k_{off}^s) for IGF-I/IGFBP-3 binding was determined as a function of k_{on}^s and K_D^s . The association rate constant (k_{on}^p) for IGF-I/p9 HS binding was varied and the dissociation rate constant (k_{off}^p) for IGF-I/p9 HS binding was determined as a function of k_{on}^p and K_D^p .

The FORTRAN program used for the Complex BAE Cell System Model can be found in Appendix B. Results for the Complex BAE Cell System Model are presented as a ratio of the ligand-receptor cell surface complexes (C) unbound receptors (Ro) present in the system as C/Ro. Most results are presented on a log scale. Base system parameters are denoted with an open diamond.

Initial analysis of the Complex BAE Cell System Model was performed with a time proceeding from 0-5 hours, (Figure 5-34). This system reaches steady state in 8 minutes. As seen with the previous model, this is much faster than seem experimentally. This may be to neglected cell effects such as IGFBP-3 and/or p9 HS cell surface binding, p9 HS secretion and IGF-I and IGF-IR secretion or degradation.



The remainder of the Complex BAE Cell System Model analysis was done at a steady state time period of 3 hours, initial ligand concentration (L_0) of 5.7×10^{-10} M, IGFBP-3 concentration (S_0) of 2.8×10^{-9} M and p9 HS concentration (P_0) of 1.4×10^{-10} M. These were chosen to mimic experimental conditions, (See Section 2.J). The system is insensitive to cell radius and ligand diffusivity, (Figure 5-35, Figure 5-36).

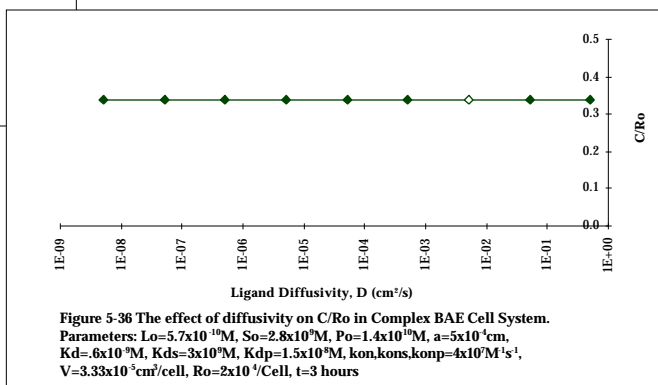
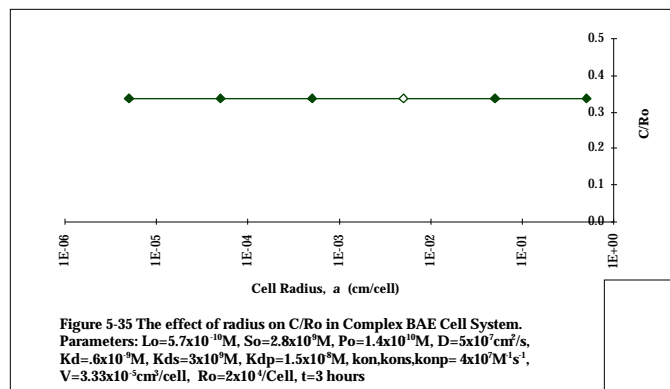
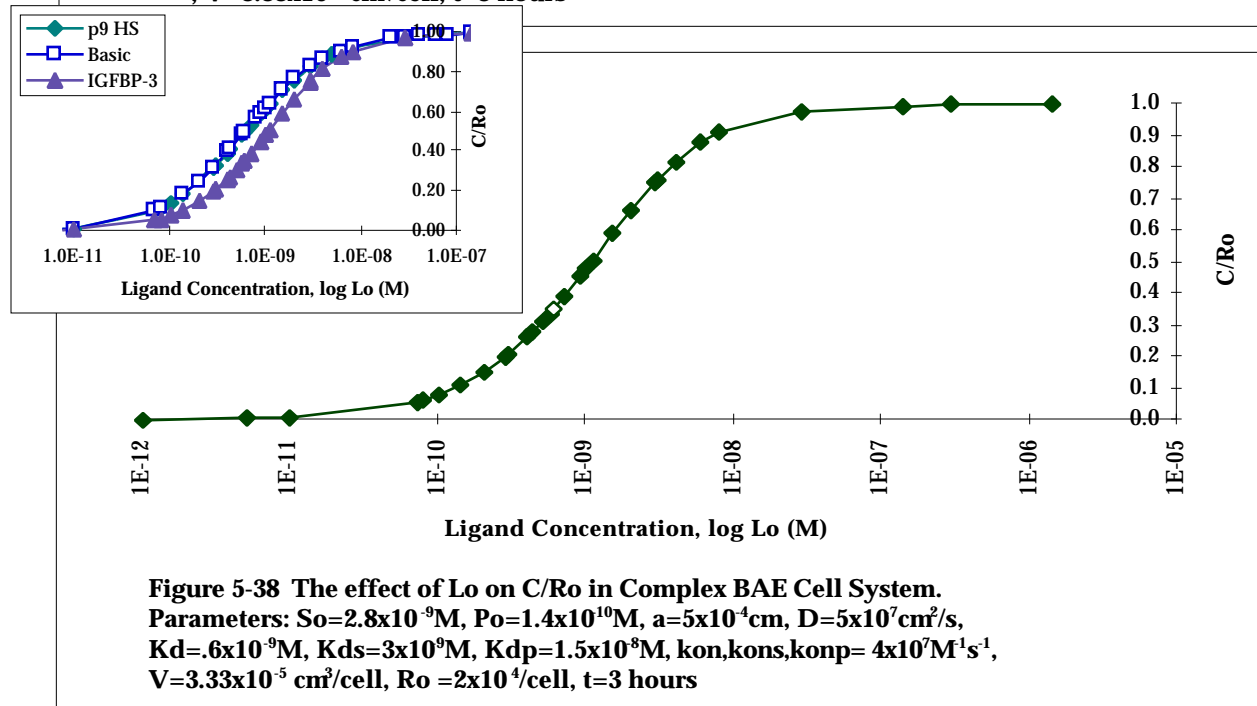
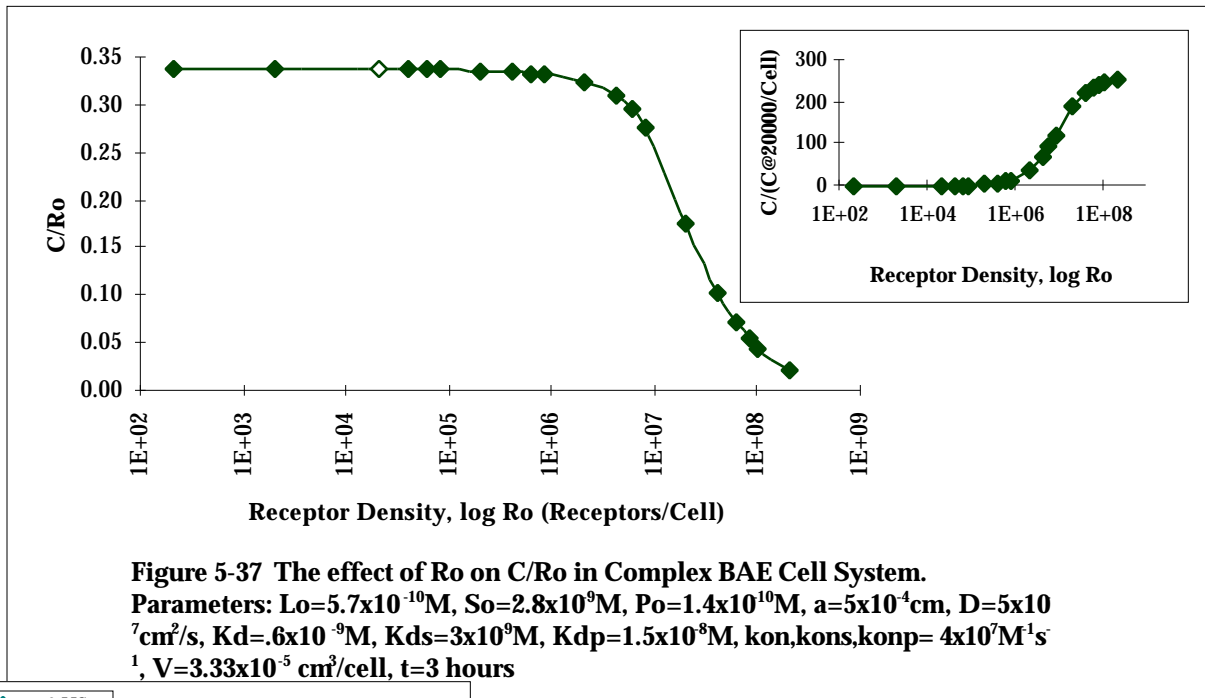


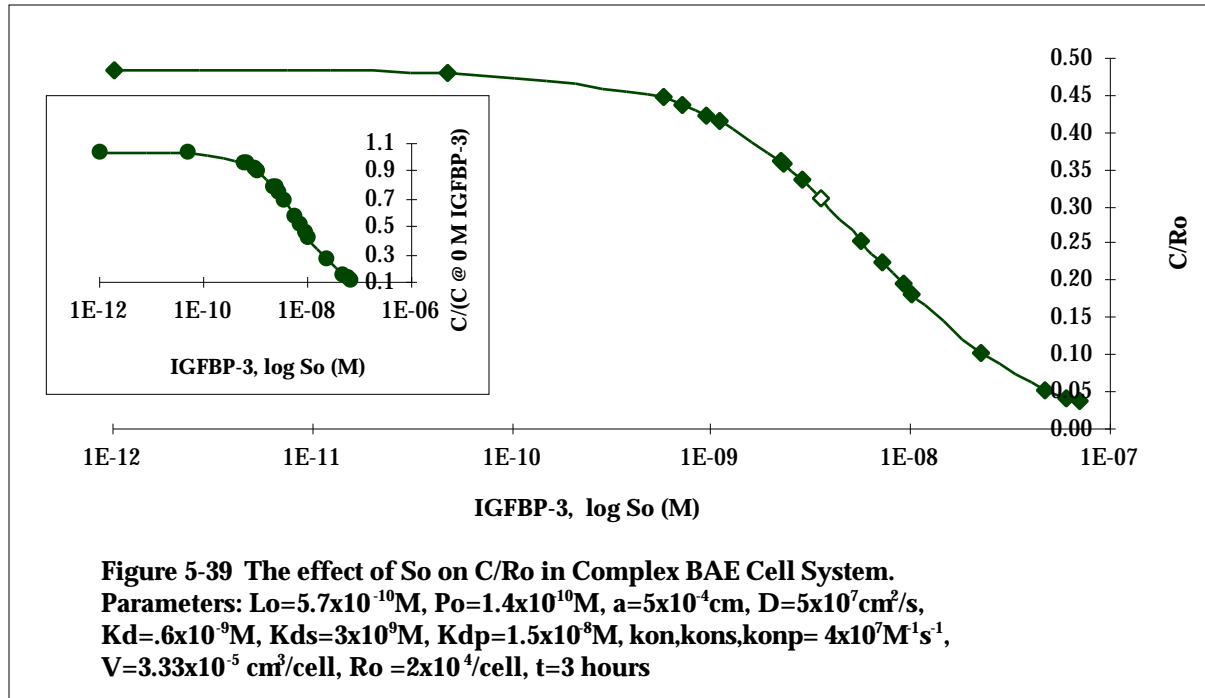
Figure 5-37 shows that as the number of available receptors on the cell surface increases from 2×10^8 - 2×10^{10} receptors/cell, the receptor occupancy (C/R_0) decreases. The decreasing effect of receptor density on C/R_0 is similar to the previous models. The half maximal decrease in this system is exactly the same as the previous systems (2×10^7 receptors/cell). The decrease of C/R_0 does not represent a decrease in surface complexes as seen in the inset of Figure 5-37. As receptor density increases, surface complexes increase.

The effect of ligand concentration (L_0) on C/R_0 is presented in Figure 5-38. There are few surface complexes predicted at very low ligand concentrations (1×10^{-12} - 1×10^{-11} M). There is an increase in C/R_0 as L_0 increases from 7.1×10^{-11} M to 2.9×10^{-8} M with a half-maximal increase at 1×10^{-9} M. The increase levels off at molar concentrations

exceeding 1.4×10^{-7} M at C/Ro equal to 1, indicating that all free receptors are bound. This also occurred with the previous models. The Basic BAE Cell System Model increase of C/Ro plateaus an order of magnitude faster than this model. This may be due to the presence of exogenous IGFBP-3 and p9 HS which force the system to require a greater ligand concentration to reach maximal C/Ro .



Exogenous IGFBP-3 (S_o) has a decreasing effect on C/R_o at all values observed, (Figure 5-39). The half-maximal decrease occurs at an IGFBP-3 concentration of 5.6×10^{-9} M. This is exactly the same response as the IGF-I/IGFBP-3 BAE Cell System Model which suggest that p9 HS is either not as effective as a soluble receptor as IGFBP-3 or not present in a concentration that is able to affect the response of the system.



Exogenous p9 HS does not affect C/R_o until p9 HS is present at high concentrations (2×10^{-9} M - 1×10^{-7} M) where surface complexes are slightly inhibited. Increasing p9 HS concentration, as a soluble receptor in the system, has less of a decreasing effect on C/R_o than IGFBP-3, as a soluble receptor, which may be due to the higher binding affinity of IGFBP-3 and IGF-I than p9 HS and IGF-I, (Figure 5-40). This model is affected with a decrease of C/R_o , in response to increasing p9 HS concentration, an order of magnitude greater than the IGF-I/p9 HS BAE Cell System. This may suggest that the presence of IGFBP-3 slows the decreasing effect of C/R_o as p9 HS increases.

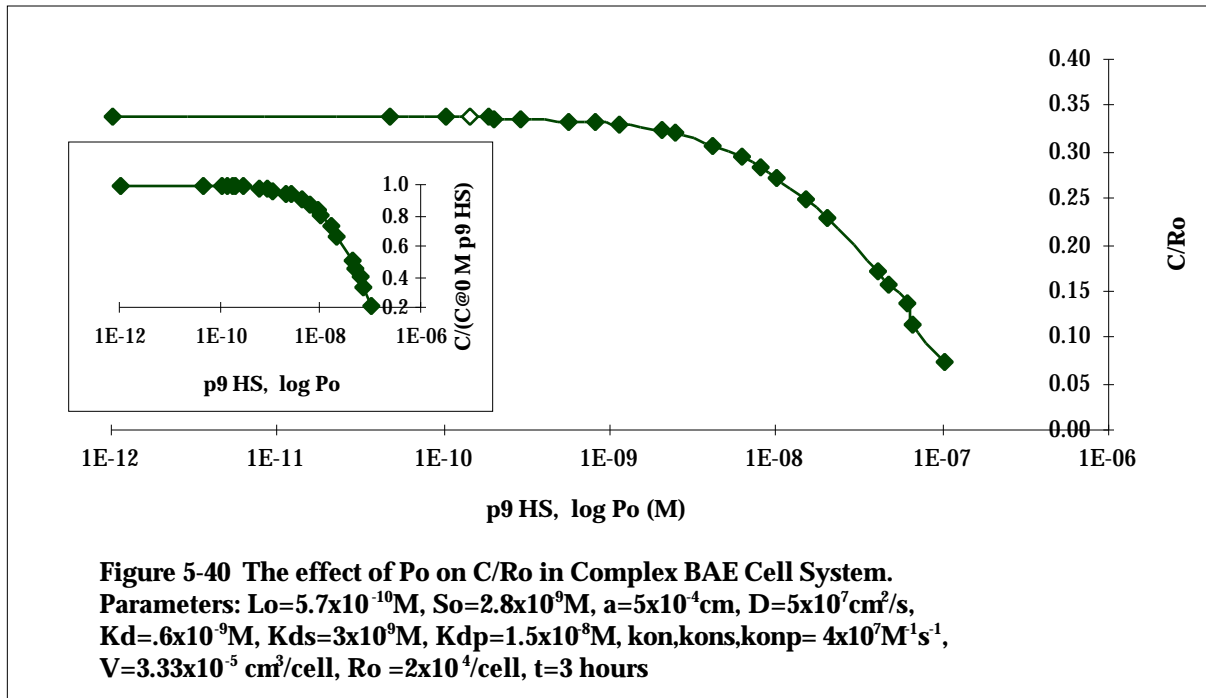
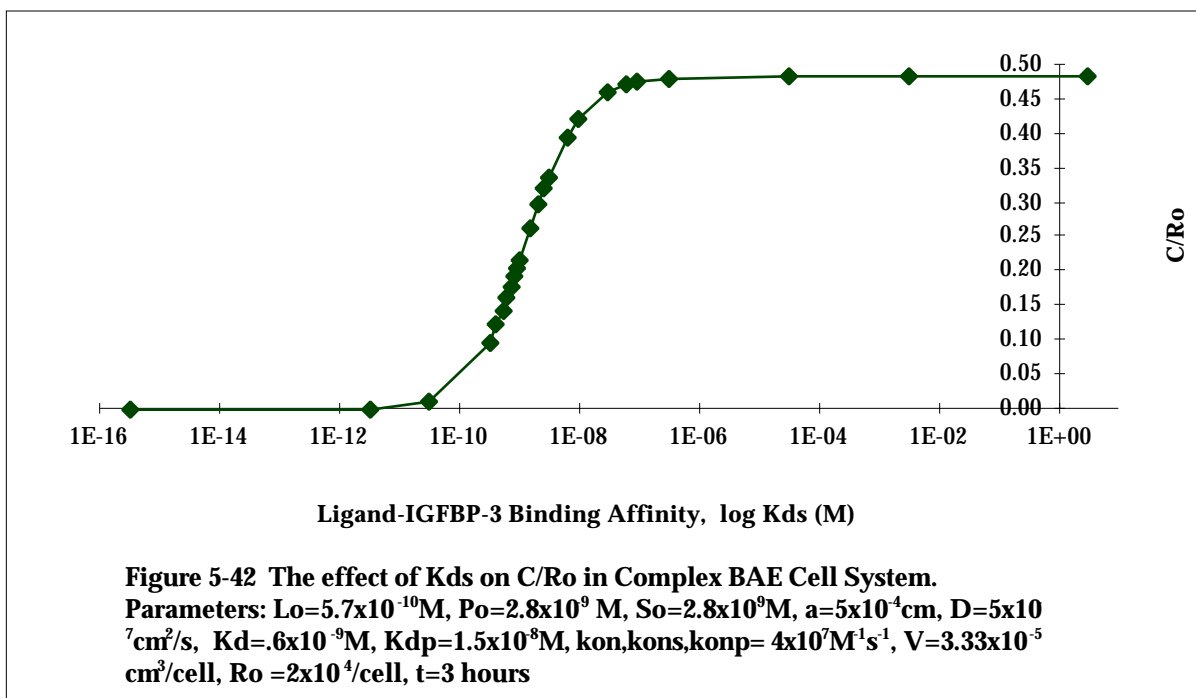
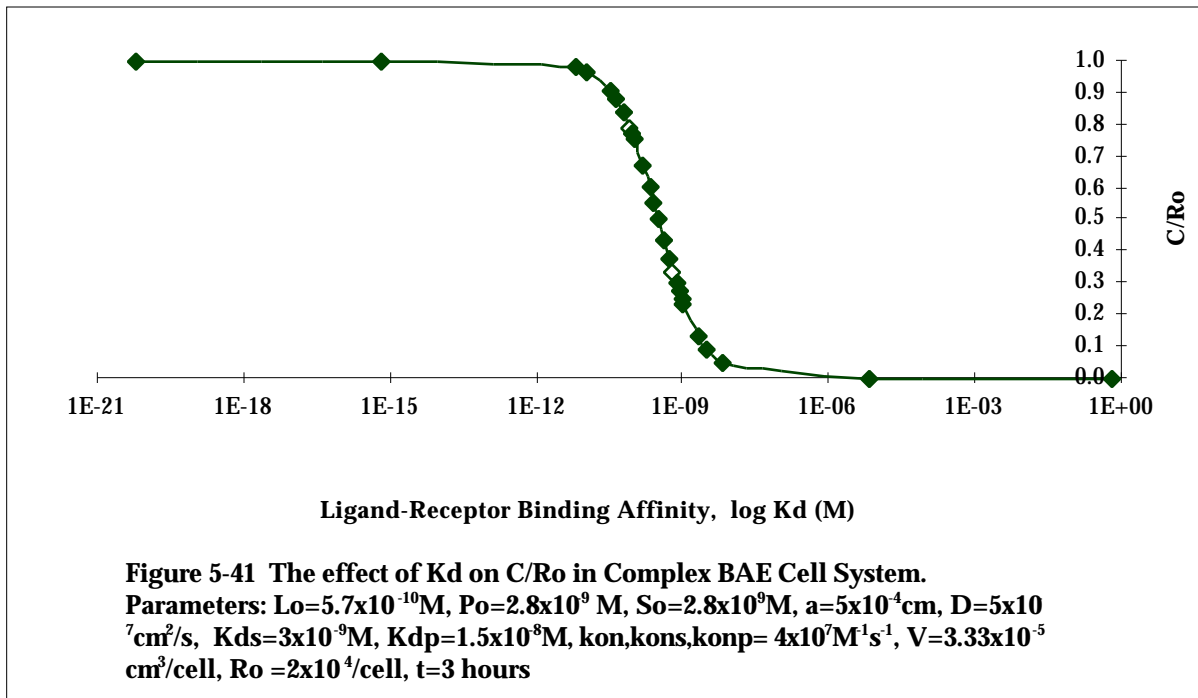


Figure 5-41 demonstrates the effect of ligand-receptor binding affinity (K_D) on C/R_0 . As K_D increases from $6 \times 10^{-21} \text{M}$ to $6 \times 10^{-12} \text{M}$, no decrease of surface complexes is predicted. C/R_0 starts to decrease at $1 \times 10^{-11} \text{M}$ and continues through $6 \times 10^{-9} \text{M}$ with a half maximal decrease occurring at $3 \times 10^{-10} \text{M}$. A low amount of surface complexes is predicted when K_D falls below $6 \times 10^{-6} \text{M}$. This is a similar trend to the previous models which suggests that IGFBP-3 and p9 HS do not alter the BAE Cell System when present together.

The effect of increasing IGF-I/IGFBP-3 binding affinity, K_D^s , on C/R_0 can be seen in Figure 5-42. At extremely high values of K_D^s ($3 \times 10^{-16} \text{M}$ - $3 \times 10^{-11} \text{M}$), few surface complexes are predicted. At these values, IGFBP-3 has a higher binding affinity for IGF-I than IGF-IR ($K_D = .6 \times 10^{-9} \text{M}$) and probably will inhibit IGF-I from reaching the surface. As binding affinity decreases from $3 \times 10^{-11} \text{M}$ to $9 \times 10^{-8} \text{M}$, C/R_0 increases significantly with a half-maximal increase at $1.25 \times 10^{-9} \text{M}$. The increase of C/R_0 levels off at $3 \times 10^{-7} \text{M}$ and reaches essentially the same level of C/R_0 as seen with the previous models. This system plateaus two orders of magnitude less than the IGF-I/IGFBP-3 BAE Cell System Model.



The effect of increasing IGF-I/p9 HS binding affinity, K_D^s , on C/R_o can be seen in Figure 5-43. As the binding affinity decreases from $1.5 \times 10^{-11} \text{ M}$ to $5 \times 10^{-9} \text{ M}$, C/R_o increases slightly with a half maximal increase occurring at $1.5 \times 10^{-10} \text{ M}$. The increase of C/R_o levels off at $1.5 \times 10^{-8} \text{ M}$. This system is less sensitive to K_D^p than K_D^s . This agrees with the idea that IGFBP-3 and p9 HS are not cooperating to affect the Complex BAE Cell System Model. The responses to this system, with both IGFBP-3 and p9 HS, are similar to the independent systems. This model predicts that IGFBP-3 and p9 HS have independent effects on IGF-I/IGF-IR binding.

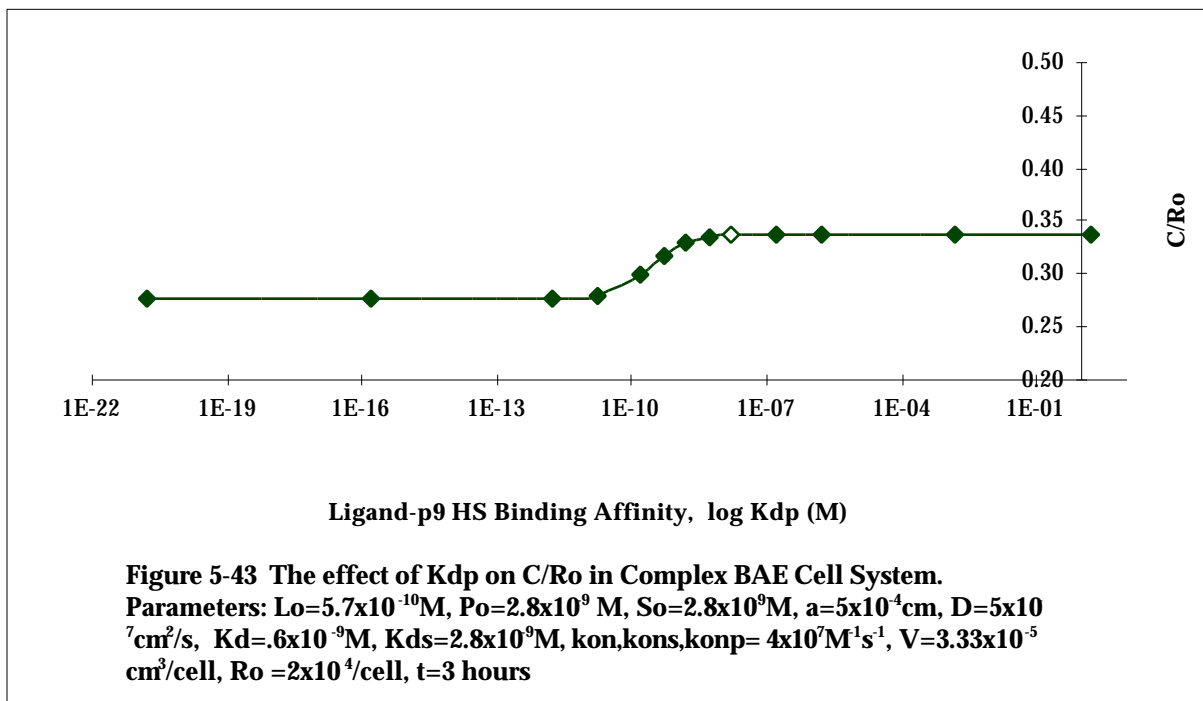


Figure 5-44 shows the effect of the variation of the association rate constant, k_{on} ($4 - 4 \times 10^{20} \text{ M}^{-1}\text{s}^{-1}$) on C/R_o while maintaining a constant K_D . As expected, at low association rate constants, k_{on} , C/R_o is very low also. Few surface complexes are predicted between k_{on} values of $4 - 4 \times 10^2 \text{ M}^{-1}\text{s}^{-1}$. Surface complexes may form at the low k_{on} values, but not last through the time period of three hours. This may be due to corresponding high dissociation rate constants (k_{off}) at low association rate constants. C/R_o starts to increase gradually at an association rate constant, k_{on} , of $1 \times 10^4 \text{ M}^{-1}\text{s}^{-1}$ and continues through $4 \times 10^5 \text{ M}^{-1}\text{s}^{-1}$. The increase plateaus at $4 \times 10^6 \text{ M}^{-1}\text{s}^{-1}$. The half-maximal increase occurs at $9 \times 10^4 \text{ M}^{-1}\text{s}^{-1}$. This is the same response as seen with the previous models.

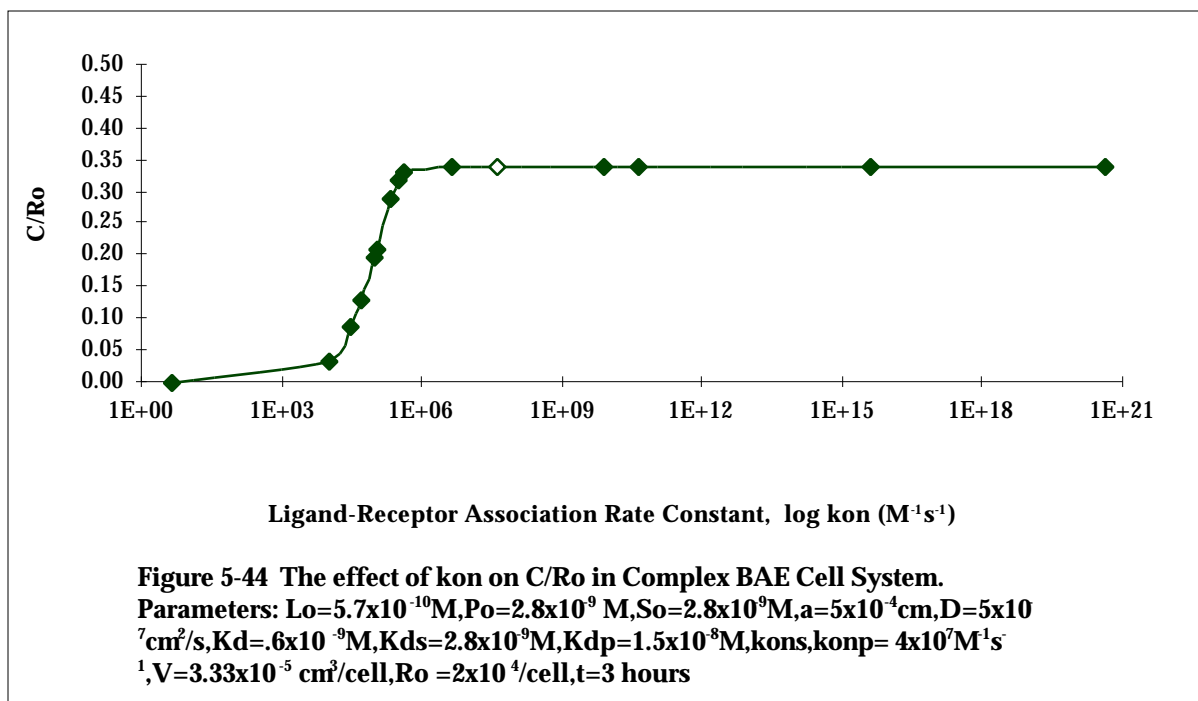


Figure 5-45 shows the effect of the ligand/IGFBP-3 association rate constant, k_{on} , on C/R_o . As k_{on} increases ($4 - 4 \times 10^{20} M^{-1}s^{-1}$), there is an overall decrease of surface complexes. However, the response of this system differs from the previous systems in that there are several intermediate plateaus and that the overall decrease is much greater. No change in surface complexes are seen when k_{on} is low ($4 - 4 \times 10^1 M^{-1}s^{-1}$). The first decrease occurs when the ratio of k_{on} ($4 \times 10^2 M^{-1}s^{-1}$) to the base case k_{on} ($4 \times 10^7 M^{-1}s^{-1}$) is 1×10^{-5} and IGF-I/p9 HS complexes are greater than IGF-I/IGFBP-3 complexes. The first decrease plateaus when the ratio of k_{on} ($4 \times 10^5 M^{-1}s^{-1}$) to the base case k_{on} ($4 \times 10^7 M^{-1}s^{-1}$) is 1×10^{-2} and IGF-I/IGFBP-3 complexes are approximately equal to IGF-I/p9 HS complexes. The second decrease begins at $1 \times 10^9 M^{-1}s^{-1}$ and a $k_{on}/k_{on, base case}$ ratio of 10 where IGF-I/IGFBP-3 complexes are greater than IGF-I/p9 HS complexes. This system predicts either a complete inhibition of surface complexes or a very fast dissociation rate of IGF-I from IGF-IR as k_{on} increases significantly ($4 \times 10^{16} M^{-1}s^{-1} - 4 \times 10^{20} M^{-1}s^{-1}$).

The effect of increasing the IGF-I/p9 HS association rate constant, k_{on} , on C/R_o can be seen in Figure 5-46. As k_{on} increases from $4 M^{-1}s^{-1}$ to $8 \times 10^9 M^{-1}s^{-1}$, C/R_o does not change. The decrease begins at $9 \times 10^9 M^{-1}s^{-1}$. As with k_{on} , the overall decrease of C/R_o

is much greater than in the previous systems. This system predicts either a complete inhibition of surface complexes or a very fast dissociation rate of IGF-I from IGF-IR as k_{on}^p increases significantly ($4 \times 10^{20} \text{ M}^{-1}\text{s}^{-1}$).

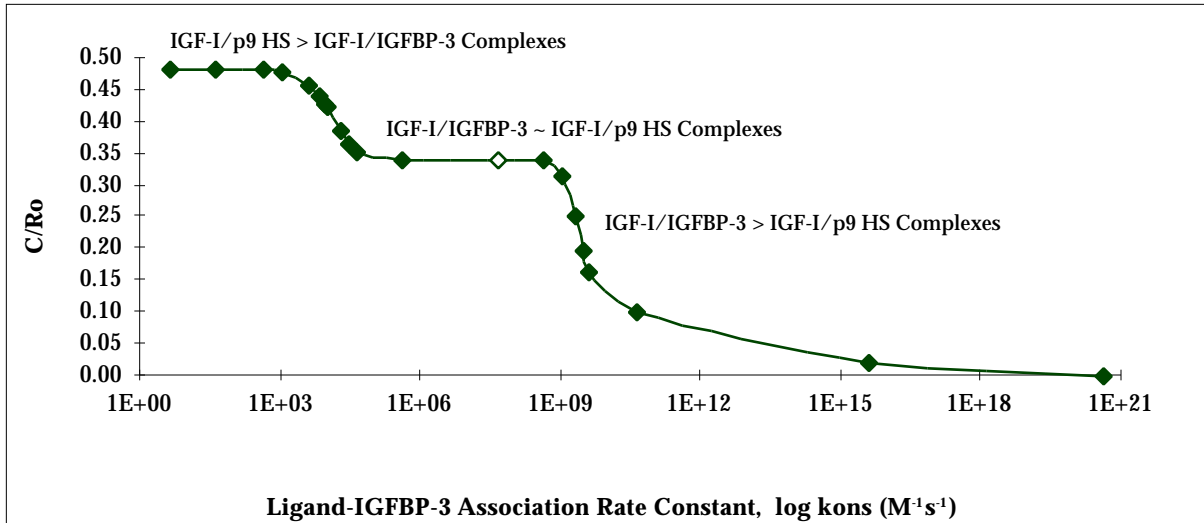


Figure 5-45 The effect of k_{ons} on C/R_o in Complex BAE Cell System.
Parameters: $L_o=5.7 \times 10^{-10} \text{ M}$, $P_o=2.8 \times 10^{-9} \text{ M}$, $S_o=2.8 \times 10^9 \text{ M}$, $a=5 \times 10^{-4} \text{ cm}$, $D=5 \times 10^7 \text{ cm}^2/\text{s}$, $K_d=.6 \times 10^{-9} \text{ M}$, $K_{ds}=2.8 \times 10^9 \text{ M}$, $K_{dp}=1.5 \times 10^8 \text{ M}$, $k_{on}, k_{onp}=4 \times 10^7 \text{ M}^{-1}\text{s}^{-1}$, $V=3.33 \times 10^{-5} \text{ cm}^3/\text{cell}$, $R_o=2 \times 10^4/\text{cell}$, $t=3 \text{ hours}$

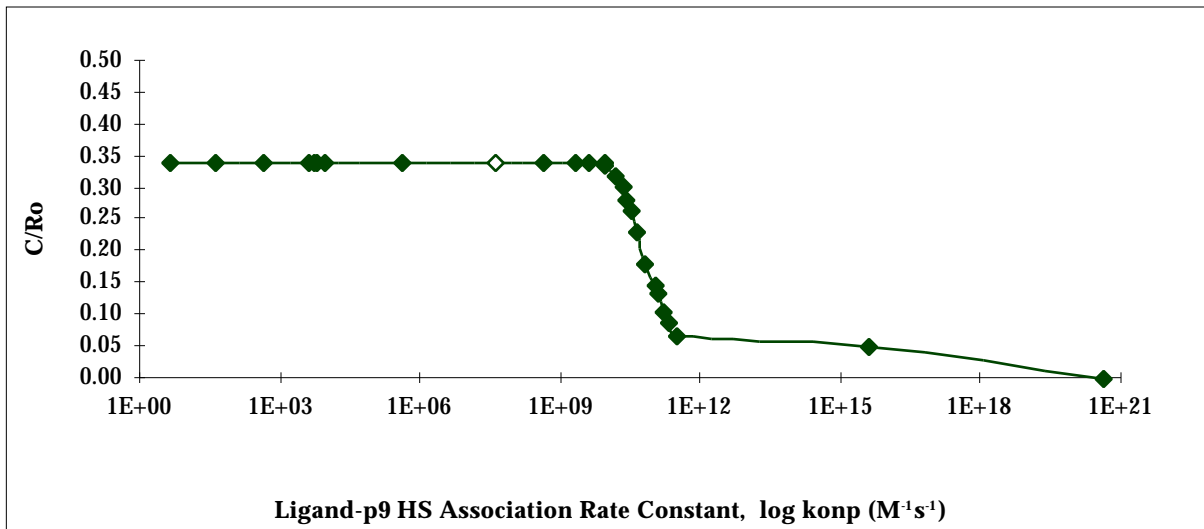
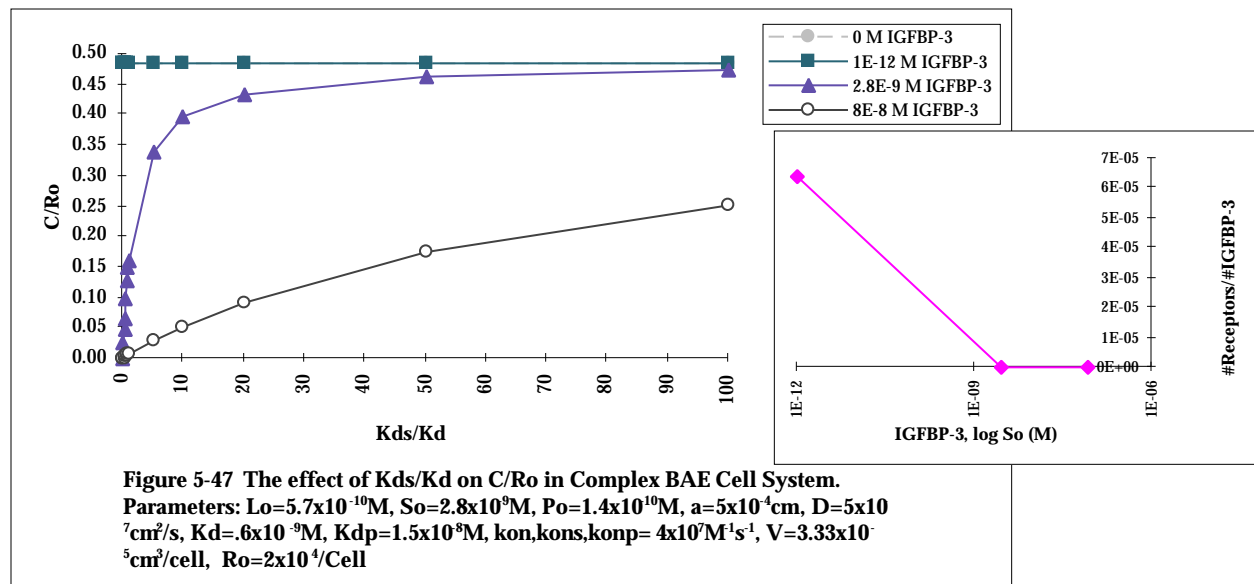
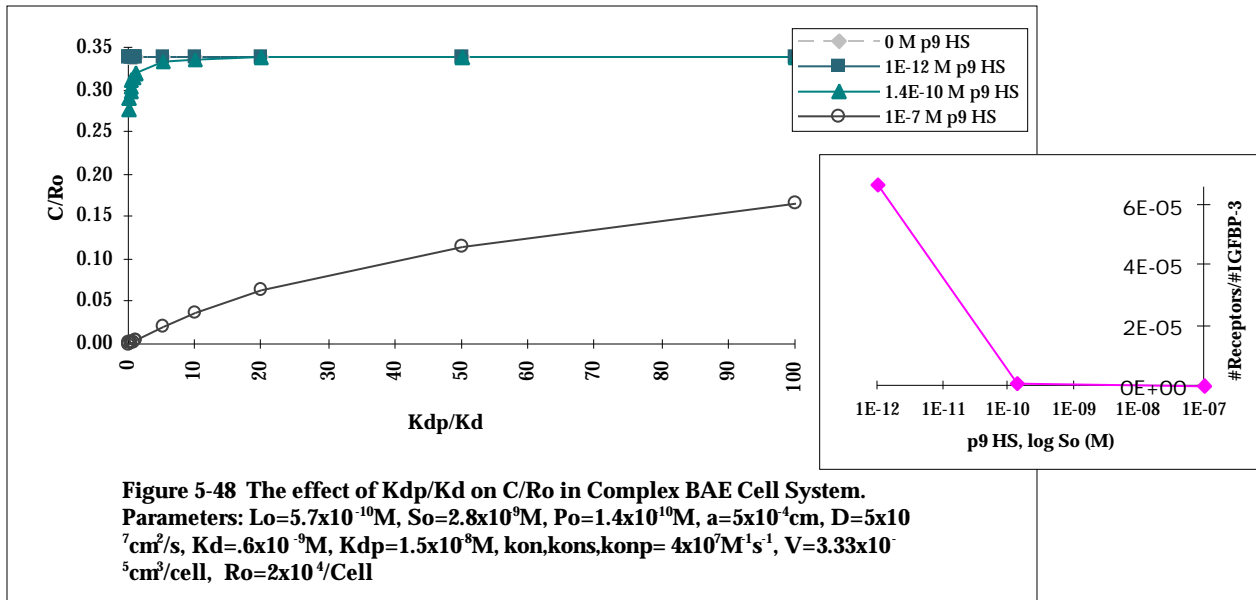


Figure 5-46 The effect of k_{onp} on C/R_o in Complex BAE Cell System.
Parameters: $L_o=5.7 \times 10^{-10} \text{ M}$, $P_o=2.8 \times 10^{-9} \text{ M}$, $S_o=2.8 \times 10^9 \text{ M}$, $a=5 \times 10^{-4} \text{ cm}$, $D=5 \times 10^7 \text{ cm}^2/\text{s}$, $K_d=.6 \times 10^{-9} \text{ M}$, $K_{ds}=2.8 \times 10^9 \text{ M}$, $K_{dp}=1.5 \times 10^8 \text{ M}$, $k_{on}, k_{ons}=4 \times 10^7 \text{ M}^{-1}\text{s}^{-1}$, $V=3.33 \times 10^{-5} \text{ cm}^3/\text{cell}$, $R_o=2 \times 10^4/\text{cell}$, $t=3 \text{ hours}$

The ratio of K_D^s to K_D , does not affect surface complexes when low concentrations of IGFBP-3 ($0 - 1 \times 10^{-12}$ M) are present in the system. Surface complexes experience an overall decrease of C/R_o when IGFBP-3 concentrations are comparable or greater than the IGF-I present in the system, as compared to the system with low concentrations of IGFBP-3, and as K_D^s/K_D increases C/R_o increases, (Figure 5-47). This may be due to decreased free receptor availability. The inset of Figure 5-47 shows that as IGFBP-3 concentration increases, the ratio of the number of receptors to the number of IGFBP-3 decreases. This is the same result as seen with the IGF-I/IGFBP-3 BAE Cell System Model.



Increasing the ratio of K_D^s to K_D , has little effect on C/R_o for p9 HS concentration similar or less than the IGF-I in the system, (Figure 5-48). Surface complexes experience an overall decrease of C/R_o when p9 HS concentrations are much greater than the IGF-I present in the system, as compared to the system when low concentrations of p9 HS are present. The inset of Figure 5-48 shows that as p9 HS concentration increases, the ratio of the number of receptors to the number of p9 HS decreases which may explain the overall decrease in surface receptor complexes. As K_D^s/K_D increases with high concentrations of p9 HS present in the system, C/R_o increases. This model requires a higher concentration of p9 HS than IGFBP-3 to result in an overall decrease of C/R_o and an increasing trend with increasing K_D^s/K_D .



The increase in receptor density, R_o , IGFBP-3 concentration, S_o , p9 HS concentration, P_o , IGF-I/IGF-IR equilibrium constant, K_D , and IGF-I/IGFBP-3 and IGF-I/p9 HS association rate constants, k_{on}^s and k_{on}^p , result in a decrease of C/R_o . An increase in ligand concentration, L_o , IGF-I/IGFBP-3 and IGF-I/p9 HS binding affinity, K_D^s and K_D^p , and the ligand-receptor association rate constant, k_{on} , results in an increase of C/R_o . An increase in K_D^s/K_D^p results in an increase in surface complexes at high concentrations of p9 HS present in the system. Surface complexes were unaffected by increasing K_D^s/K_D^p and K_D^p/K_D^s when low concentrations of IGFBP-3 or p9 HS are present. An increase of both the IGF-I/IGFBP-3 and IGF-I/p9 HS association rate constants, k_{on}^s and k_{on}^p , result in a decrease of C/R_o that is greater than seen with the IGF-I/IGFBP-3 and IGF-I/p9 HS BAE Cell System Models. The system reaches steady state in eight minutes.

The Complex BAE Cell System Model predicts that IGFBP-3 and p9 HS act independently as soluble receptors in the system. There was little difference in all the parameters varied as compared with the previous systems. This indicates that there is no interaction between the two soluble receptors. This is in contrast to what was seen experimentally. This may be due to the neglect of soluble receptor surface binding. Later experiments have indicated that IGFBP-3 and p9 HS do bind to the surface.

B. Model/Experimental Comparisons:

Qualitative comparisons can be made between the models and experimental data for IGF-I surface complexes when exposed to levels of soluble receptors.

The IGF-I/IGFBP-3 BAE Cell System Model predicts an overall decrease of surface complexes as exogenous IGFBP-3 increases, (Figure 5-15). Experimental data presented in Chapter IV, Figure 4-4 verifies that increasing IGFBP-3 ($4.7 \times 10^{-10} \text{ M}$ - $2.2 \times 10^{-8} \text{ M}$) decreases that amount of IGF-I that binds to the cell surface. The model predicts that there is no change in surface complexes at IGFBP-3 concentrations of $4.7 \times 10^{-10} \text{ M}$ - $5.6 \times 10^{-10} \text{ M}$. This agrees with the experimental data where lower molar concentrations of IGFBP-3 (4.7×10^{-10} - $5.6 \times 10^{-10} \text{ M}$) do not affect the level of surface complexes seen experimentally. The model predicts that surface complexes begin to decrease at $7 \times 10^{-10} \text{ M}$ exogenous IGFBP-3. A decrease in surface complexes was experienced at $2.8 \times 10^{-9} \text{ M}$ experimentally. The IGF-I/IGFBP-3 BAE Cell System Model predicts the behavior of the experimental system successfully. However, later experiments have shown that surface binding of IGFBP-3 does occur, however, IGFBP-3/IGFBP-3R binding affinity has not been quantified, (Figure 4-9). This may affect C/Ro ratio values, but it is doubtful that it will affect the overall trends seen in the model.

The IGF-I/p9 HS BAE Cell System Model predicts an overall decrease of surface complexes as exogenous p9 HS increases, (Figure 5-27). Experimental data presented in Chapter IV, Figure 4-5 contradicts the model predictions. The addition of p9 HS ($1 \times 10^{-10} \text{ M}$ - $8 \times 10^{-10} \text{ M}$) increases IGF-I binding to BAE cells. The disagreement between the model and the experimental data is likely due to the assumption that there is no p9 HS surface binding. Later experiments have shown that p9 HS does bind to the surface, however, results have not been quantified, (Figure 4-10).

The Complex BAE Cell System Model predicts a decrease in surface complexes when IGFBP-3 concentration ($1 \times 10^{-12} \text{ M}$ - $7 \times 10^{-8} \text{ M}$) increases in the presence of p9 HS ($1.4 \times 10^{-10} \text{ M}$), (Figure 5-39). The trend agrees with the experimental data discussed in Chapter IV, Figure 4-8. However, experimental data shows that when IGFBP-3 is present at low concentrations ($5 \times 10^{-11} \text{ M}$ - $6 \times 10^{-10} \text{ M}$) and p9 HS is also present (2 - $8 \times 10^{-10} \text{ M}$), there is an increase of surface complexes as compared to the system with no

IGFBP-3 or p9 HS. The Complex BAE Cell System Model does not show any increase at low concentrations of IGFBP-3. This is more than likely due to the neglect of IGFBP-3 and p9 HS surface binding.

The Complex BAE Cell System Model predicts that with an increasing concentration of p9 HS ($1 \times 10^{-12} \text{ M}$ - $1 \times 10^{-7} \text{ M}$) in the presence of IGFBP-3 ($2.8 \times 10^{-9} \text{ M}$), there is a decrease in the number of surface complexes. This does not agree with experimental data discussed in Chapter IV, Figure 4-7. Experimental data showed that an increase of p9 HS ($5 \times 10^{-12} \text{ M}$ - $2 \times 10^{-10} \text{ M}$) in the presence of IGFBP-3 (2.8×10^{-9}) increased IGF-I surface binding as compared to the system with no p9 HS present. Again, this is more than likely due the simplifying assumption for the model that there is no p9 HS surface binding.

C. Future Direction

The models discussed do not predict experimental results successfully likely due to the surface binding of IGFBP-3 and p9 HS. A future model is being developed to account for soluble receptors binding to the surface, (Figure 5-49). IGFBP-3 and p9 HS bind to their own surface receptors, RS and RP, respectively. K_D^D and K_D^E represent the binding affinities of IGFBP-3/RS and p9 HS/RP. The forward and reverse rate constants for IGFBP-3/RS binding and p9 HS/RP binding are $k_{\text{for}}^D/k_{\text{rev}}^D$ and $k_{\text{for}}^E/k_{\text{rev}}^E$, respectively. Lack of experimental data to quantify the binding affinity of IGFBP-3 and p9 HS to the surface prevents model discussion at this point. It has been shown that IGFBP-3 binds to a different class of cell surface receptors than IGF-I. The class of IGFBP-3 surface receptors, the transmembrane domain and the capacity for signaling has yet to be determined³⁹. IGFBP-3 has direct cellular effects that are independent of IGF-I³⁹.

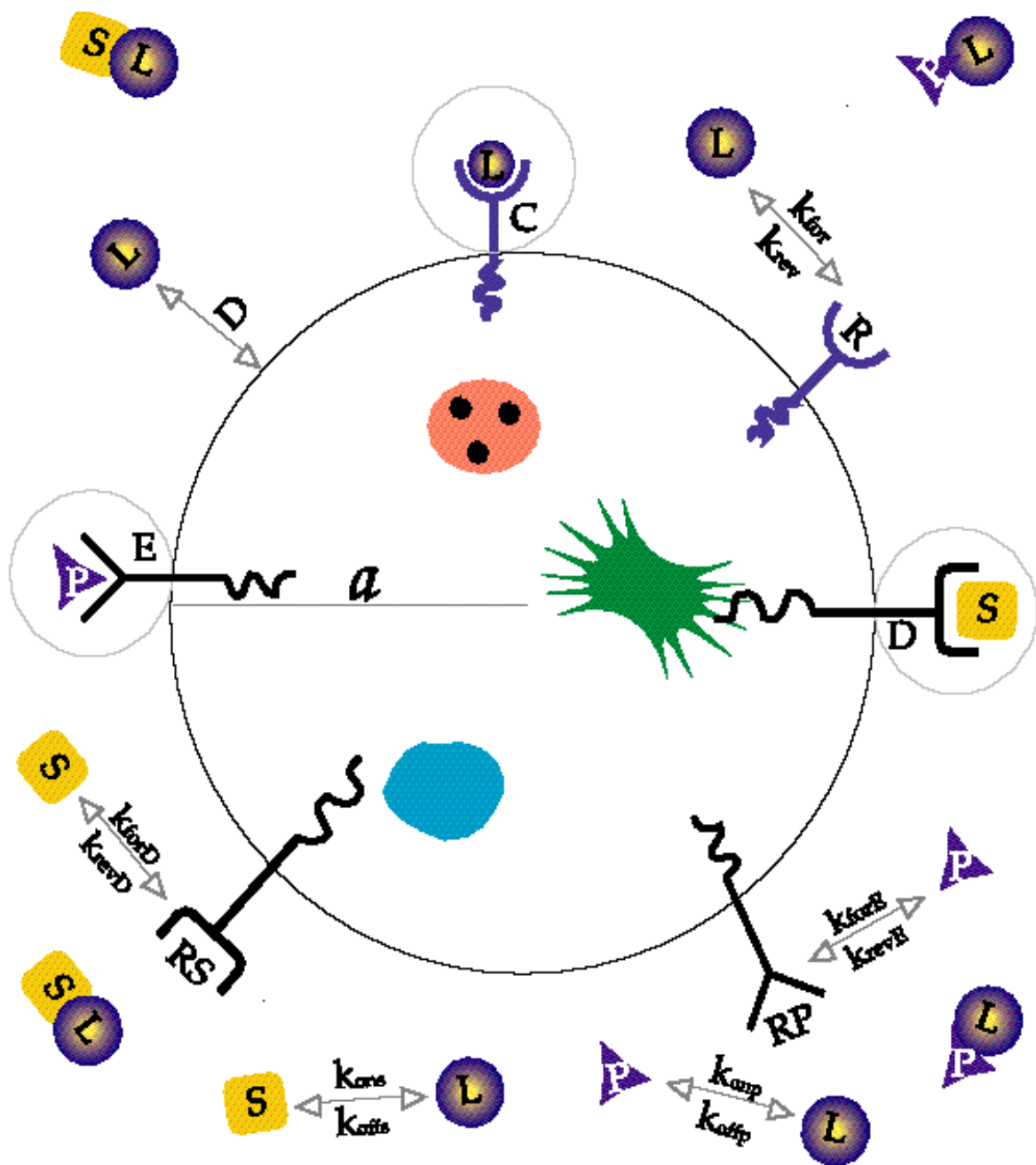


Figure 5-49 Schematic illustration of Future Complex BAE Cell System Model.
All variables and parameters are described by symbol in the text.